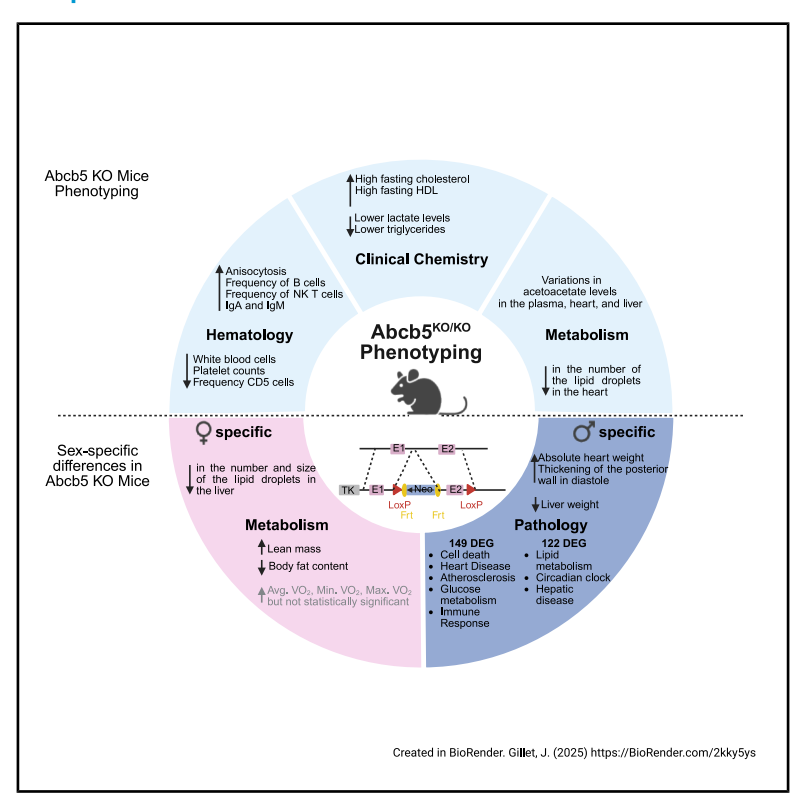
# **iScience**

# Abcb5-deficient mice show a subtle, pleiotropic phenotype indicating a role for this transporter in intermediary metabolism

## **Graphical abstract**



#### **Authors**

Jean-Pierre Gillet, Louise Gerard, Wilfred Vieira, ..., Lino Tessarollo, Di Xia, Michael M. Gottesman

## Correspondence

jean-pierre.gillet@unamur.be (J.-P.G.), gottesmanm@mail.nih.gov (M.M.G.)

#### In brief

Physiology; Cell biology; Cancer

## **Highlights**

- Abcb5-deficient C57BL/6J mice were generated by deleting exon 2 and are fertile
- Mice exhibit metabolic changes, anisocytosis, and reduced WBC and platelet counts
- Marked sex differences in body composition, calorimetry, heart, and liver
- No single Abc compensates for Abcb5 loss; multiple show variable upregulation





**iScience** 



### **Article**

# Abcb5-deficient mice show a subtle, pleiotropic phenotype indicating a role for this transporter in intermediary metabolism

Jean-Pierre Gillet, <sup>1,11,\*</sup> Louise Gerard, <sup>1</sup> Wilfred Vieira, <sup>2</sup> Marie Fourrez, <sup>1</sup> Florence Gaudray, <sup>1</sup> Birgit Rathkolb, <sup>3,4,5</sup> Jan Rozman, <sup>3,4,6</sup> Tanja Klein-Rodewald, <sup>3</sup> Lore Becker, <sup>3</sup> Antonio Aguilar-Pimentel, <sup>3</sup> Marion Horsch, <sup>3</sup> Nadine Spielmann, <sup>3</sup> Cornelia Prehn, <sup>3,10</sup> Benoît Bihin, <sup>7</sup> Johannes Beckers, <sup>3,4,8</sup> Helmut Fuchs, <sup>3</sup> Valérie Gailus-Durner, <sup>3</sup> Martin Hrabe de Angelis, <sup>3,4,8</sup> Eileen Southon, <sup>9</sup> Lino Tessarollo, <sup>9</sup> Di Xia, <sup>2</sup> and Michael M. Gottesman<sup>2,\*</sup>

#### **SUMMARY**

ABCB5 is a member of the ATP-binding cassette transporter superfamily that is expressed as a full transporter (ABCB5FL) and half transporter (ABCB5β). The ABCB5FL transporter mediates low-level multidrug resistance in cancer and is normally expressed in the prostate and testis, while ABCB5β has been found to be a marker of melanoma and limbal stem cells and is expressed in pigmented cells. To explore ABCB5's role in normal physiology, we generated Abcb5-deficient C57BL/6J mice by the deletion of Abcb5 exon 2, knocking out both forms of ABCB5, which were completely phenotyped. The mice were fertile and demonstrated altered bioenergetics and fat metabolism, along with alterations in their blood composition, including anisocytosis and decreased white blood cells and platelet counts. This study uncovers further avenues of investigation into the role of Abcb5 in intermediary metabolism, particularly in relation to atherogenesis.

#### **INTRODUCTION**

ABCB5 is a member of the 48 ATP-binding cassette (ABC) transporter superfamily encoded by the human genome. In humans, 11 different ABCB5 transcript variants have been identified, including ABCB5.b² and ABCB5.a, both of which give rise to transporters. ABCB5.b, which is also referred to as ABCB5β, is a half transporter that must either homo- or heterodimerize to be functional; it is found to be predominantly expressed in melanocytes. ABCB5.a, which is also referred to as ABCB5FL (full length), is a typical ABC transporter comprising two transmembrane domains and two nucleotide-binding domains; it has been shown to confer multidrug resistance in cancer 1,5 and has been documented solely in the prostate and testis.

Phylogenetic and evolutionary analyses have shown that ABCB5 evolved as a full transporter for most of its evolutionary history and is most closely related to the other full transporters of its family: ABCB1, ABCB4, and ABCB11. ABCB5 has been reported as a marker of skin progenitor cells, melanoma-initiating cells, and, more recently, as a marker of limbal stem cells. Furthermore, ABCB5 mutations are commonly found in melanoma. In a recent study, we showed that ABCB5 was mutated in approximately 14% of the 640 melanoma samples analyzed. Biochemical ATPase activity assays have demonstrated that mutations lead to either a decrease or loss of function of the protein, which, in turn, accelerates the development of melanoma. We speculate that once this transporter is no longer functional, physiological changes occur that affect cell metabolism and/or mutagenesis related to toxic reactive oxygen species.



<sup>&</sup>lt;sup>1</sup>Laboratory of Molecular Cancer Biology, URPhyM, NARILIS, Faculty of Medicine, University of Namur, 5000 Namur, Belgium

<sup>&</sup>lt;sup>2</sup>Laboratory of Cell Biology, Center for Cancer Research, National Cancer Institute, NIH, Bethesda, MD 20892-4256, USA

<sup>&</sup>lt;sup>3</sup>Institute of Experimental Genetics and German Mouse Clinic, Helmholtz Zentrum Munchen, German Research Center for Environmental Health, 85764 Neuherberg, Germany

<sup>&</sup>lt;sup>4</sup>German Center for Diabetes Research (DZD), 85764 Neuherberg, Germany

<sup>&</sup>lt;sup>5</sup>Institute of Molecular Animal Breeding and Biotechnology, Gene Center, Ludwig-Maximilians-University München, 80539 Munich, Germany <sup>6</sup>Institute of Molecular Genetics of the Czech Academy of Sciences, Czech Centre for Phenogenomics, Prumyslova 595, 252 50 Vestec, Czech Republic

<sup>&</sup>lt;sup>7</sup>NARILIS, University of Namur, Scientific Support Unit, CHU UCL Namur, 5530 Godinne, Belgium

<sup>&</sup>lt;sup>8</sup>Chair of Experimental Genetics, TUM School of Life Sciences, Technische Universität München, 85354 Freising, Germany

<sup>&</sup>lt;sup>9</sup>Mouse Cancer Genetics Program, Center for Cancer Research, NCI-Frederick, Frederick, MD 21702-1201, USA

<sup>&</sup>lt;sup>10</sup>Present address: Metabolomics and Proteomics Core, Helmholtz Zentrum München, German Research Center for Environmental Health, 85764 Neuherberg, Germany

<sup>&</sup>lt;sup>11</sup>Lead contact

<sup>\*</sup>Correspondence: jean-pierre.gillet@unamur.be (J.-P.G.), gottesmanm@mail.nih.gov (M.M.G.) https://doi.org/10.1016/j.isci.2025.113617





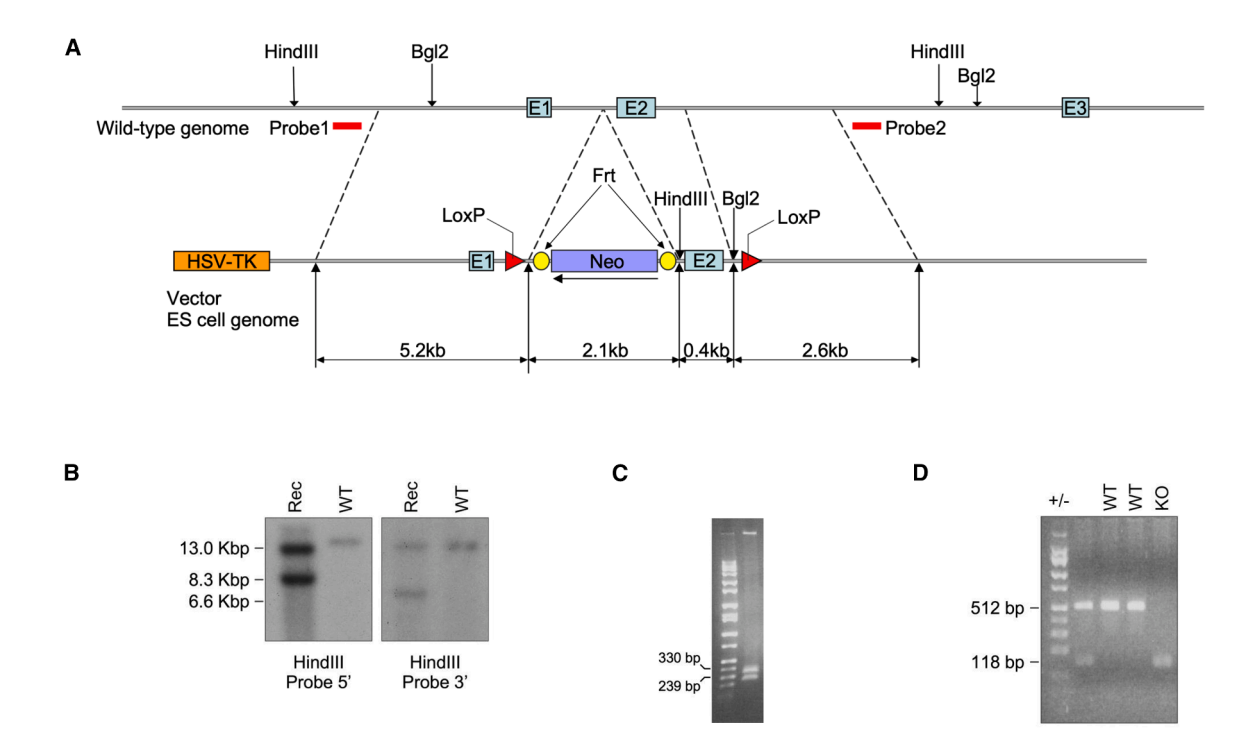


Figure 1. Conditional deletion of Abcb5 in mice

(A) Schematic representation of the strategy used to target the Abcb5 gene. LoxP sites (red triangles) were inserted upstream and downstream of exon 2 (E2). The neomycin resistance cassette (NEO) is flanked by Frt sites (yellow ovals).

(B) After the initial screening of the positive ES cell clones, a 5' external probe (red rectangle) was used to identify the targeted alleles by detecting a shift from the endogenous HindllI wild-type (WT) band of 13 kb to the rearranged 8.7 Kb band resulting from the insertion of the *neo* cassette by homologous recombination. The correct targeting was confirmed by using a 3' external probe following digestion with the HindllI restriction enzyme, which detects a shift from the 13 Kb endogenous WT band to the rearranged 6.6 Kb mutant band. HSV-TK, thymidine kinase cassette for the negative selection; pBS, backbone pbluescript vector. (C) The presence of the distal *loxP* site in the genome was tested by PCR. Amplification of the WT or mutant Abcb5 alleles resulted in bands of either 239 bp (WT) or 330 bp (recombined allele).

(D) Mice were routinely genotyped by isolating genomic DNA from an ear punch using 100 ng of genomic DNA as the template. Amplification of the WT or mutant Abcb5 alleles resulted in bands of either 512 bp ( $Abcb5^{+/+}$ ) or 112 bp ( $Abcb5^{-/-}$ ).

In the current study, we explore the normal physiological function of Abcb5. To do this, the Abcb5 knockout mouse line was generated by the deletion of Abcb5 exon 2. Mutant mice were derived from hybrid 129/Sv-C57BL/6J embryonic stem cells injected into C57BL/6J blastocysts and were backcrossed for at least six generations onto the C57BL/6J background before use. Mice deficient in Abcb5 expression were fertile and harbored a subtle, pleiotropic phenotype, indicating a role for this transporter in intermediary metabolism.

#### **RESULTS**

#### **Generation of Abcb5-knockout mice**

The mouse ortholog of ABCB5FL (Chromosome 7, NC\_000007.14, NM\_001163941.2), Abcb5 (Chromosome 12, NC\_000078.7, NM\_029961.2), encodes a 1255 amino acid protein with all the structural features of a typical ABC transporter, which has two transmembrane domains and two nucleotide binding domains (NBDs). All the expected NBD motifs, including Walker A, Walker B, the C loop, and the Q loop, are present in the NBDs, and they are completely canonical in their sequences (Figure S1).

To explore the physiological function of this transporter, exon 2 of the Abcb5 gene was targeted in mouse embryonic stem (ES) cells by a standard replacement-type targeting vector constructed by microhomologous recombination in bacteria, 12 here using an 8.2 Kb C57BL/6J mouse genomic fragment retrieved by the Bacterial Artificial Chromosome (BAC) RP23-161L22 (Figure 1A).<sup>13</sup> Electroporation and selection were performed using the v6.4 ES cell line, as described by Southon and Tessarollo.14 DNAs derived from G418/FIAU resistant ES clones were screened by diagnostic HindIII restriction enzyme digestions using, respectively, a 5' and 3' probe external to the targeting vector sequence (Figure 1B). Recombinant clones containing the predicted rearranged band were obtained at a frequency of 4/10. Two independently targeted ES cell clones injected into C57BL/6J blastocysts generated chimeras that transmitted the mutated allele to the progeny. 15 Following the germline transmission of the targeted ES cell clones, the diagnostic HindIII digest was used for screening because it enabled us to distinguish between the wild-type (WT) and all targeted alleles, including those generated after Cre or Flpe recombination. The presence of the distal LoxP site in the genome was





Table 1. Body composition analysis in female and male Abcb5 WT and Abcb5 KO mice

	Female		Male		Linear model			
	WT	WT KO		WT KO		Sex	Body mass	Sex:Genotype
	N = 10	N = 10	N = 10	N = 10				
	Mean ± sd	Mean ± sd	Mean ± sd	Mean ± sd	p-value	p-value	p-value	p-value
Body mass	21.3 ± 2.1	21.6 ± 1.6	29.9 ± 2.9	28.8 ± 2.4	0.511	<0.001	NA	0.334
Fat mass	5.4 ± 1	$4.9 \pm 0.7$	$6.8 \pm 0.7$	$6.9 \pm 0.8$	0.807	0.061	< 0.001	0.004
Lean mass	12.7 ± 1.2	$13.4 \pm 0.8$	19.1 ± 1.9	18 ± 1.5	0.432	0.005	<0.001	0.003

Means, standard deviation, and p-values of a linear model.

confirmed before crossing with the  $\beta\text{-}\mathrm{actin}\text{-}\mathrm{cre}$  mice, which express a transgene expressing Cre recombinase directed by the human  $\beta\text{-}\mathrm{actin}$  gene promoter (Figure 1C). The mice were then genotyped using PCR (Figure 1D). Mutant mice were backcrossed for at least six generations onto the C57BL/6J background before use.

# Abcb5-deficient mice harbor altered bioenergetics and fat metabolism

The German Mouse Clinic (GMC) screen comprises extensive phenotyping based on standardized methods (Tables S1 and S2). <sup>16–18</sup> Two cohorts, each with 10 male and 10 female WT and homozygous mutant adult mice and all born within one week, were subjected to the GMC phenotyping program between the ages of 8 and 17 weeks (Tables S1 and S3). The result overview is presented in Table S4.

During the 21-h indirect calorimetry trial, no major mutation effect was detected on energy metabolism parameters. Mean and minimum oxygen consumption were only slightly increased in female mutants when adjusted for body mass. Interestingly, stronger differences were observed regarding maximum oxygen consumption, which was increased in the female mutants (Table S5). Body mass did not significantly differ between the control and mutant mice. Time domain nuclear magnetic resonance scans for body composition analysis also did not reveal any significant main effects of genotype on body fat content and lean mass. However, a significant sex-genotype interaction was found in females both for body fat content (p < 0.004) and lean mass (p < 0.003). Females showed slightly decreased fat content and increased lean mass, whereas in males, no difference between genotypes was observed (Table 1).

Clinical chemistry analysis revealed that the Abcb5-deficient mice had lower lactate levels compared with their WT counterparts (p < 0.01) (Table 2; Figure 2A). Interestingly, after overnight food withdrawal, we observed higher cholesterol levels in mutant mice (p = 0.046) (Figure 2B), especially high-density lipoprotein (HDL) cholesterol (p = 0.028) (Table 3; Figure 2C). On the other

hand, non-HDL cholesterol levels, including low-density lipoprotein (LDL) and very low-density lipoprotein (VLDL) cholesterol, were slightly increased, but not statistically significant (p = 0.217) (Table 3). In samples from ad libitum-fed mice, we did observe a statistically significant decrease in plasma triglyceride values in the mutant mice (p = 0.016) (Table 4; Figure 2D).

# Abcb5-deficient mice show an increased anisocytosis and a higher frequency of B and NK-T cells

Blood sample analysis of Abcb5-mutant mice showed an increased anisocytosis, as indicated by elevated red blood cell distribution width (RDW) values (p = 0.012), as well as decreased white blood cell (p = 0.004) and platelet counts (p = 0.001) in the mutant mice (Table S6). FACS analysis uncovered a higher frequency of B cells (p = 0.036), together with a lower frequency of CD5 coexpressing cells within the B cell cluster (B1-cells, p = 0.011). Moreover, analysis revealed a slightly higher frequency of NK-T cells (NK+CD5+) in peripheral blood from the mutants (p = 0.044) (Table S7). The immunoglobulin screening uncovered higher levels of IgA (p = 0.006) and IgM (p = 0.012) in the blood plasma of mutant mice compared with the controls (Table S8).

# Male Abcb5-deficient mice present a decrease in liver weight and an increase in heart weight

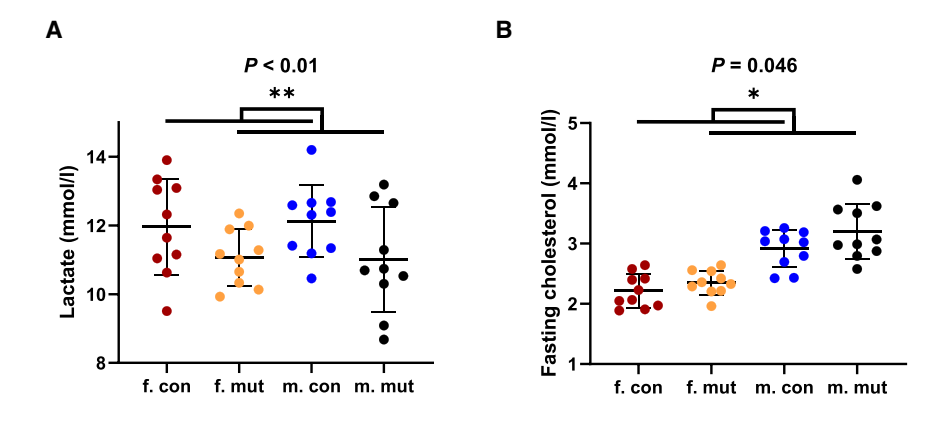
Interestingly, the macroscopical analysis of visceral organs revealed a decrease in liver weight when using body weight as a covariate (Figure 3A), as well as a male-specific increase in absolute heart weight (Figure 3B). However, no alterations in visceral organs were detected in histological analysis. Representative images of mice's heart and liver are shown in Figures 3C and 3D. Notably, the basal cardiovascular functions were investigated by awake echocardiography, which revealed a thickening of the posterior wall in diastole in mutant mice. This observation was found to be statistically significant in mutant males (p = 0.011) (Table S9). No substantial changes in the interventricular septum in systole (IVSs), interventricular septum in diastole

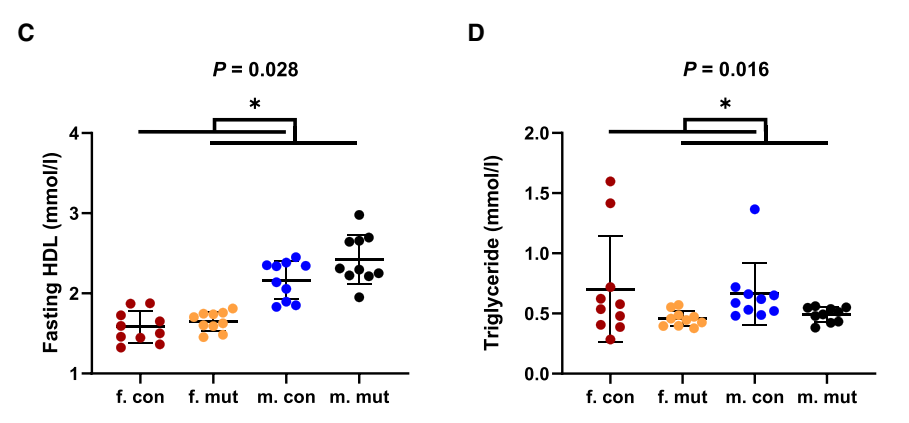
Table 2. Lactate levels [mmol/L] in female and male Abcb5 WT and Abcb5 KO mice

	Female		Male		Linear model			
	WT	KO	WT		Genotype	Sex	Sex:Genotype	
	N = 10	N = 10	N = 10	N = 10				
	Mean ± sd				p-value			
Lactate [mmol/L]	11.97 ± 1.4	11.07 ± 0.82	12.12 ± 1.05	11 ± 1.52	0.01	0.91	0.77	









(IVSd), left ventricular posterior wall in systole (LVPWs), left ventricular internal dimension in systole (LVIDs), and left ventricular internal dimension in diastole (LVIDd) were observed between wild type and mutant mice in echocardiography (Table S9).

Since Abcb5-deficient mice present a decreased triglyceride level and because the heart and liver are the key altered organs in these mice, the heart and liver lipid content of WT mice and Abcb5-deficient mice were analyzed. Lipid droplets were stained using Oil Red O dye. Abcb5-deficient mice showed a reduced number of lipid droplets in the heart (p = 0.011), a female-specific decrease in droplet number in the liver (p = 0.021), and a female-specific decrease in droplet size in the liver (p = 0.019) (Figure 4).

Gene expression profiling was performed on the hearts and livers taken from four male mutant mice and four WT mice at the age of 18 weeks. Three out of four mutant livers showed a strong correlation in gene expression. Statistical analysis carried out on these three mutant samples identified 122 significantly differentially regulated genes between mutant and control livers (Data S1). The estimated number of falsely significant genes was calculated for 1,000 permutations, yielding a false discovery rate (FDR) of 1.7%. Differentially regulated genes in the liver are associated with lipid metabolism (Stard4, Thrsp, Insig1, Insig2, Apom, Arntl, Atg3), circadian clock (Ccrn4l, Dbp, Tef, Fgf21, Nfil, Per2), and hepatic disease (Cops, Id1, Wnt2, Usp2) (Table S10). A similar analysis of four mutant hearts identified 149 differentially expressed

Figure 2. The Abcb5-mutant mice have lower lactate levels, indicating a shift in cellular energy metabolism

(A) Lactate levels [mmol/L] in female (f) and male (m) Abcb5+/+ (control, con) and Abcb5-/- (mutant, mut) mice. Reduced lactate levels were detected in the ABCB5-/- mice (p < 0.01), Table 2.

(B) Fasting cholesterol boxplot with stripchart, split by sex and genotype ( $\rho = 0.046$ ), Table 3. (C) Fasting HDL cholesterol boxplot with strip-

(C) Fasting HDL cholesterol boxplot with strip-chart, split by sex and genotype (p = 0.028), Table 3.

(D) Triglyceride boxplot with stripchart, split by sex and genotype (p=0.016), Table 4. Two cohorts, each consisting of 10 male and 10 female WT and homozygous mutant adult mice, all born within one week, were subjected to clinical chemistry analyses at 13 and 14 weeks of age. Means, standard deviations, and p-values for genotype, sex, and genotype–sex interaction effects were calculated using a linear model. \*p<0.05, \*\*p<0.01, \*\*\*p<0.001.

genes with an FDR of 0.6% (Data S2). These genes were associated, for instance, with cell death (Ahsp, Ang, Cdkn1a, Thra, Timp1), heart disease (Bnip3l, Ca2, Col3a1, Csf3r, Fos, Gpx1, Il1b, Lep, Prkag2, Rorc, Thra, Timp1, Uts2), atherosclerosis (Cdkn1a, Fos, Il1b, Lep, Lgals3, S100a8, S100a9, Timp1), glucose metabolism (Ca2, Ccdc68, Cdkn1a, Dbh, E2f2, Fah, Gpx1, Hbb,

II1b, Lep), and immune response (IL1B, ISG20, LEP, LGALS3, LGALS4, MPP1, S100A8, S100A9) (Table S11).

#### Abcb5-deficient mice show altered ketone body levels

Since the subtle phenotype observed in Abcb5-deficient mice suggests a role for this transporter in metabolism, ketone bodies were quantified in the plasma, heart, and liver of Abcb5-deficient mice compared to WT mice. Ketone bodies (acetoacetate, acetate,  $\beta$ -hydroxybutyrate) are produced in the liver in response to decreased glucose availability to supply energy to various organs, including the heart. <sup>19</sup> Variations in acetoacetate levels were observed in the liver (p=0.028) (Table 5; Figure 5). A female-specific decrease and a malespecific increase in  $\beta$ -hydroxybutyrate levels were observed in the heart (p=0.048) and liver (p=0.020). A similar observation was made for acetate levels in the liver (p=0.028) (Table 5; Figure 5).

#### $ER\alpha$ activates ABCB5 $\beta$ transcription

There was a marked sex difference in the various parameters observed. We therefore hypothesized that hormones regulate Abcb5 expression. Hormone response elements (HREs) exist in the Abcb5 promoter region, in particular the estrogen-response element (ERE). Therefore, the effect of human estrogen receptor alpha (hER $\alpha$ ) on the expression of ABCB5, the human homolog of Abcb5, was investigated in a luciferase reporter assay. hER $\alpha$ ,





	Female		Male		Linear model		
	WT	KO	WT	KO	Genotype	Sex	Genotype-sex
	N = 10	N = 10	N = 10	N = 10			
	Mean ± sd				p-value		
Fasting Glucose [mmol/L]	10.62 ± 1.52	12.11 ± 2.19	11.19 ± 2.74	11.11 ± 1.54	0.284	0.748	0.237
Fasting Cholesterol [mmol/L]	$2.215 \pm 0.278$	$2.352 \pm 0.201$	$2.914 \pm 0.31$	$3.203 \pm 0.46$	0.046	< 0.001	0.467
Fasting HDL Cholesterol [mmol/L]	1.581 ± 0.197	1.651 ± 0.12	2.164 ± 0.241	2.422 ± 0.308	0.028	<0.001	0.2
Fasting non-HDL Cholesterol [mmol/L]	$0.634 \pm 0.089$	0.701 ± 0.113	$0.75 \pm 0.123$	0.781 ± 0.161	0.217	0.017	0.655
Fasting Triglycerides [mmol/L]	$0.976 \pm 0.255$	1.071 ± 0.532	$1.339 \pm 0.799$	$1.032 \pm 0.364$	0.532	0.339	0.238
Fasting NEFA [mmol/L]	0.58 ± 0.11	0.66 ± 0.11	$0.6 \pm 0.14$	$0.57 \pm 0.07$	0.393	0.307	0.122
Fasting Glycerol [mmol/L]	$0.199 \pm 0.032$	0.185 ± 0.024	0.157 ± 0.028	0.159 ± 0.011	0.448	< 0.001	0.28

Means, standard deviations, and p-values for genotype, sex, and genotype–sex interaction effects calculated by a linear model.

in the presence of its ligand, estrogen, can bind to the ERE in the promoter region of its target gene to regulate its transcription. MelJuSo, a melanoma cell line known to constitutively express ABCB5,<sup>20</sup> was transfected with pSG5-hERα and either 3xERE:: luc-TATA, ABCB5β\_3xERE::luc-TATA, or ABCB5β\_0xERE::luc-TATA. 3xERE::luc-TATA is the luciferase reporter plasmid containing the gene encoding luciferase under the control of three estrogen-response elements from the vitellogenin A2 gene promoter. ABCB5β\_3xERE::luc-TATA is the luciferase reporter plasmid containing the gene encoding luciferase under the control of three estrogen-response elements from ABCB5β. ABCB5β\_0xERE::luc-TATA is the negative control lacking estrogen-response elements. When incubated with 5 mM of estrogen 24 h post-transfection, hER $\alpha$  activates ABCB5 $\beta$ \_3xERE::luc-TATA transcription while ABCB5β\_0xERE::luc-TATA luminescence is similar to that of wild-type cells (Figure 6). As expected, in the absence of estrogen, hER $\alpha$  is unable to activate luciferase transcription (Figure 6).

Since hormones regulate Abcb5 expression, plasma steroid hormone levels were determined by LC-MS/MS in both wild-type mice and Abcb5-deficient mice. Corticosterone, androstenedione, and testosterone concentrations were similar between wild-type and mutant mice (Table 6). Typical

sex-specific differences were observed for testosterone and corticosterone between male and female mice (Table 6).

# Compensation mechanism through ATP-binding cassette transporter upregulation

Abcb5 mRNA expression level was first examined in threemonth-old WT mice using RT-qPCR (Table S12). Expression was found in the thymus of all male and female animals at an average  $\Delta Ct$  of 32.84. Abcb5 was also expressed in the white adipose tissue (WAT), testis, tail skin, and muscle of all male animals examined. Remarkably, the greatest Abcb5 mRNA level was found in the white adipose tissue and testis, with an average ΔCt of 17.73 and 18.80, respectively. The expression of Abcb5 mRNA in the tail skin and muscle was lower, with an average ΔCt of 28.76 and 30.62, respectively. Abcb5 mRNA was also found in the liver, small intestine, transverse colon, and back skin in at least one of the three male animals examined, for which we obtained triplicate samples. With the exception of back skin, in which Abcb5 mRNA was found to be expressed in two out of the three animals examined, here with an average  $\Delta$ Ct of 30.58, in the other tissues, the transporter mRNA was found to be expressed in only one animal, with a  $\Delta$ Ct of 30 or greater. In

Table 4. Lipid and	glucose levels, as well as selec	ted enzyme activities in th	e plasma of ad libitum-fed mice

	Female		Male		Linear model			
	WT	KO	WT	KO	Genotype	Sex	Genotype-sex	
	N = 10 N = 10		N = 10 $N = 10$					
	Mean ± sd				p-value			
Cholesterol [mmol/L]	1.796 ± 0.245	1.853 ± 0.28	2.79 ± 0.364	2.475 ± 0.243	0.164	<0.001	0.048	
Triglyceride [mmol/L]	$0.702 \pm 0.444$	$0.458 \pm 0.065$	$0.662 \pm 0.26$	$0.492 \pm 0.062$	0.016	0.968	0.658	
ALAT/GPT [U/I]	31 ± 16	31 ± 15	22 ± 3	26 ± 7	0.529	0.058	0.461	
ASAT/GOT [U/I]	44 ± 5	$39 \pm 5$	41 ± 15	42 ± 9	0.45	1	0.326	
Alpha-Amylase [U/I]	483.36 ± 73.84	469.99 ± 59.06	560.75 ± 78.28	606.71 ± 65.99	0.464	< 0.001	0.187	
Glucose [mmol/L]	12.45 ± 2.12	12.41 ± 1.01	12.32 ± 1.81	12.03 ± 1.16	0.743	0.617	0.801	
LDH [U/I]	202.6 ± 50.2	189.2 ± 57.5	167.5 ± 38.9	177.4 ± 36.6	0.906	0.12	0.434	

Means, standard deviations, and *p*-values for genotype, sex, and genotype–sex interaction effects calculated by a linear model. ALAT/GPT: alanine-aminotransferase; ASAT/GOT: aspartate aminotransferase; LDH: lactate-dehydrogenase.



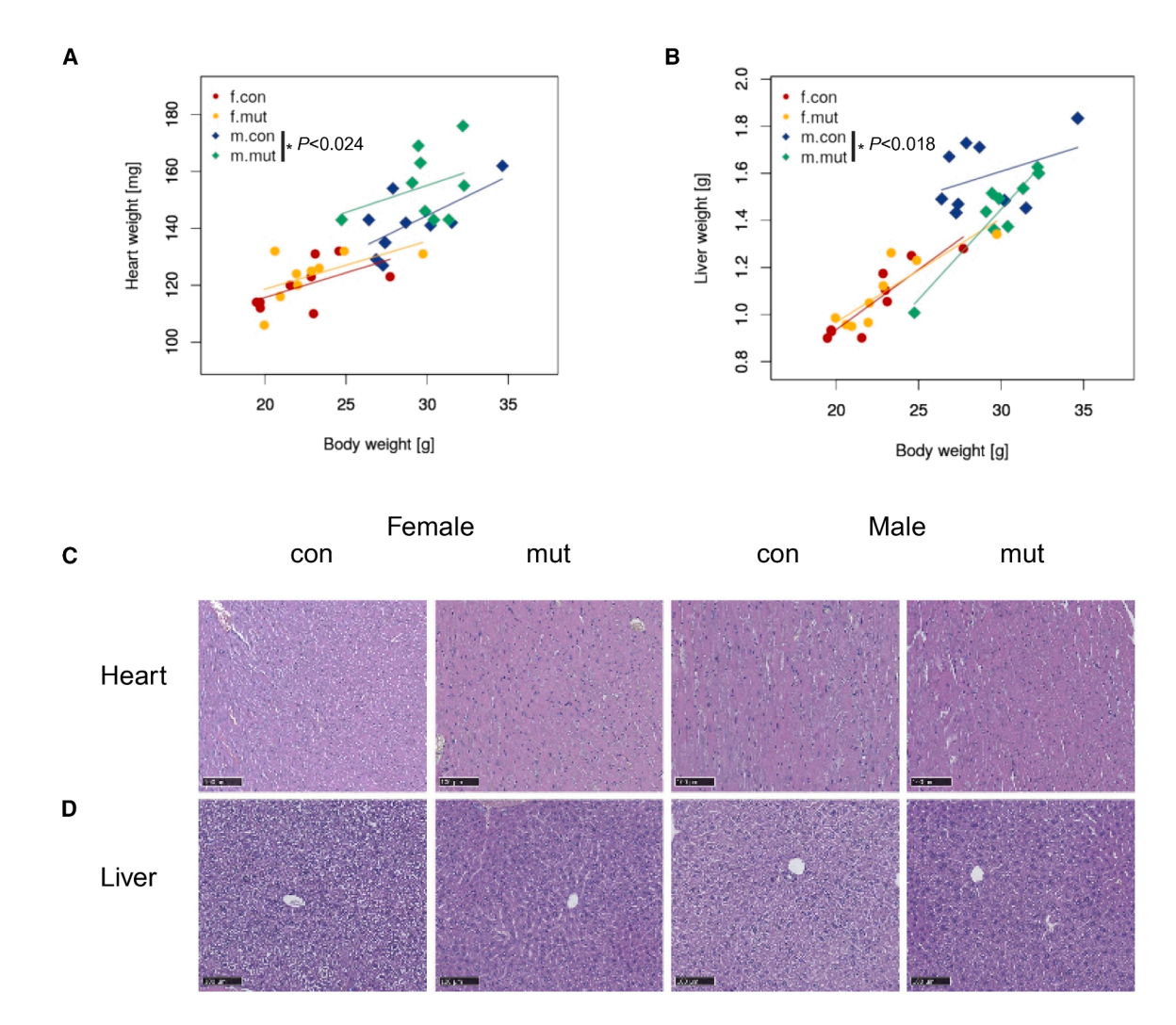


Figure 3. A male-specific increase in heart weight and a decrease in liver weight

(A) Liver weight/body weight scatterplot with regression line, split by sex (female, f; male, m) and genotype (control, con; mutant, m). A male-specific decrease in liver weight using body weight as a covariate, p < 0.018.

(B) Heart weight scatterplot with regression line, split by sex (female, f; male, m) and genotype (control, con; mutant, m). A male-specific increase in heart weight using body weight as a covariate, p < 0.024.

(C) Histological representative images of the heart from control (con) and mutant (mut) mice stained with hematoxylin and eosin.

(D) Histological representative images of the liver from control (con) and mutant (mut) mice stained with hematoxylin and eosin. Two cohorts, each consisting of 10 male and 10 female WT and homozygous mutant adult mice, all born within one week, were subjected to pathology analyses at 16 weeks of age. \*p < 0.05, \*\*p < 0.01, \*\*\*p < 0.001. Scale bar = 100  $\mu$ M.

females, Abcb5 was expressed in the ovaries of all the animals investigated, with an average  $\Delta Ct$  of 23.77. We also found Abcb5 mRNA in the brain, white adipose tissue, kidney, and tail skin in at least one of the three female animals examined, for which we have a triplicate measure.

The mRNA expression profile of the 52 other murine Abc transporters was then measured in three-month-old Abcb5<sup>-/-</sup> and age-matched WT mice to determine the effect of Abcb5 deficiency on their expression level (Table S13). We focused on the thymus, white adipose tissue, testis, ovary, and skin. Because we could observe a phenotype in the heart and liver, we decided to include these two organs in our analysis, even though we could not detect Abcb5 expression in both tissues.

Many Abc transporter genes were significantly differentially expressed in the liver (n=45/52), thymus (n=15/52), and testis (n=12/52) of Abcb5-deficient mice, in contrast to the heart (6/52), white adipose tissue (5/52), skin (5/52), and ovary (4/52) (Table S14; Figures 7 and 8). In the thymus and testis, all the Abc genes were significantly upregulated, while in the skin and ovary, they were all found to be downregulated. In the liver, 43 of the 45 Abc genes were upregulated in Abcb5-deficient mice. Among those, nine were found to be upregulated, with a fold change greater than 10.

The analysis of the Abcb family revealed that Abcb1 was upregulated in the heart and liver of Abcb5-deficient mice, while Abcb6 was overexpressed in the WAT and liver of these mice.





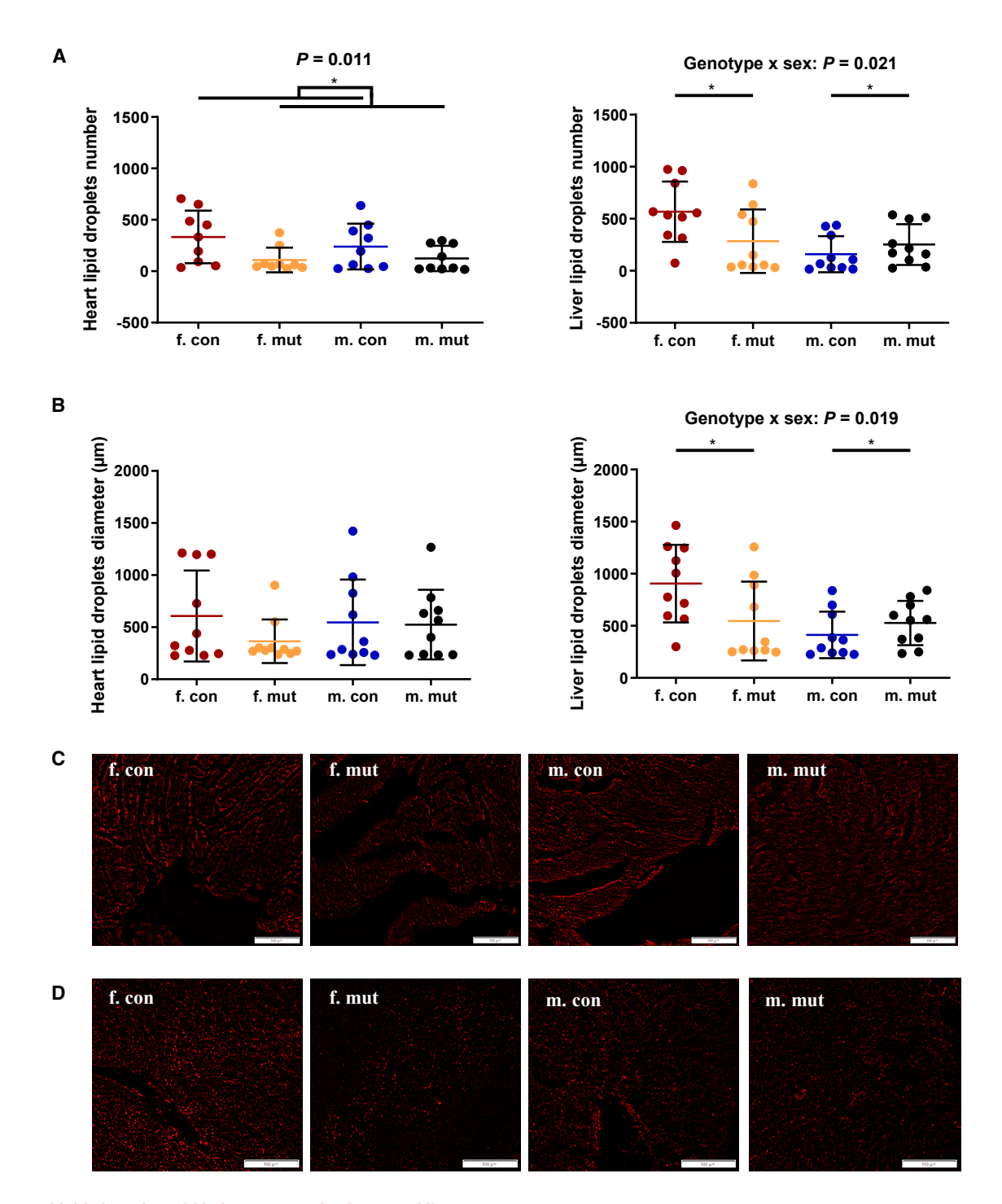


Figure 4. Lipid alteration of Abcb5-mutant mice heart and liver

(A) The number of heart and liver lipid droplets after staining with Oil Red O (n = 10). Droplets were counted using ImageJ. Abcb5-deficient mice showed a reduced number of lipid droplets in the heart (p = 0.011), and a female-specific decrease in droplet number in the liver (p = 0.021).

(B) Diameter of heart and lipid droplets after staining with Oil Red O (n = 10). The Droplets diameter was determined using ImageJ. A female-specific decrease in droplet size in the liver was observed (p = 0.019).

(C) Representative image of heart sections stained with Oil Red O.

(D) Representative image of liver sections stained with Oil Red O. Two cohorts, each consisting of 10 male and 10 female WT and homozygous mutant adult mice, all born within one week, were analyzed for heart and liver lipid content at 8 weeks of age. Means, standard deviations, and p-values for genotype, sex, and genotype–sex interaction effects were calculated using a two-way ANOVA. \*p < 0.05, \*\*p < 0.01, \*\*\*p < 0.001. Scale bar = 100  $\mu$ M.



Table 5.	Ketone body levels in t	he plasma, hea	rt, and liver of f	emale and male	Abcb5 WT and	Abcb5 KO m	ice	
		Female		Male		Linear model		
		WT	KO	WT	KO	Genotype	Sex	Genotype-sex
		N = 10	<i>N</i> = 10	<i>N</i> = 10	N = 10			
		Mean ± sd				p-value		
Plasma	Acetoacetate [mmol/L]	2.279 ± 2.320	2.464 ± 1.781	3.518 ± 2.122	$4.793 \pm 3.802$	0.393	0.042	0.523
	Acetate [mmol/L]	$6.656 \pm 5.604$	6.170 ± 4.992	$3.803 \pm 3.981$	$5.554 \pm 3.830$	0.670	0.246	0.453
	β-hydroxybutyrate [mmol/L]	3.540 ± 1.067	3.109 ± 2.110	2.681 ± 1.233	2.743 ± 2.041	0.730	0.256	0.645
Heart	Acetoacetate [mmol/L]	$23.65 \pm 10.36$	$18.30 \pm 21.06$	$8.830 \pm 7.110$	10.18 ± 5.429	0.636	0.01	0.429
	Acetate [mmol/L]	$6.586 \pm 6.785$	$6.265 \pm 4.362$	$4.547 \pm 3.194$	$6.486 \pm 3.302$	0.585	0.539	0.446
	β-hydroxybutyrate [mmol/L]	4.445 ± 1.118	3.390 ± 3.177	1.194 ± 1.295	2.686 ± 1.570	0.727	0.003	0.048
iver	Acetoacetate [mmol/L]	22.85 ± 12.27	13.07 ± 6.490	13.28 ± 10.56	10.29 ± 5.318	0.028	0.034	0.233
	Acetate [mmol/L]	31.34 ± 20.81	$18.13 \pm 7.336$	18.95 ± 20.93	$32.13 \pm 20.07$	0.998	0.890	0.028
	β-hydroxybutyrate [mmol/L]	3.786 ± 1.916	2.586 ± 0.973	2.016 ± 0.959	2.766 ± 1.155	0.579	0.055	0.020

Means, standard deviations, and p-values for genotype, sex, and genotype  $\times$  sex interaction effects calculated by a linear model.

Even though Abcb8 was upregulated in the testis and thymus of Abcb5-deficient mice, no Abcb8 mRNA could be detected in the heart and liver of these mice, which is in contrast to their WT counterparts. Finally, Abcb9, b10, and b11 were upregulated in the testis, thymus, and liver of Abcb5-deficient mice.

Overall, Abcb5 deficiency is not compensated for by the overexpression of a single ABC transporter in all seven organs analyzed. Instead, several ABC transporters were found to be upregulated with no consistency among the organs analyzed. In other words, we found different ABC transporters that were overexpressed in each organ we examined.

#### **DISCUSSION**

The role of ABCB5 in the biology of normal cells remains elusive. Here, we report the complete phenotyping of Abcb5-deficient mice that were generated by the deletion of the Abcb5 exon 2 from hybrid 129/Sv-C57BL/6J ES cells injected into C57BL/6J blastocysts. These mice were backcrossed onto the C57BL/6J background before being subjected to the GMC phenotyping program, which occurred between the ages of two and five months. The analyses revealed several statistically significant genotype-related differences associated with fat metabolism and blood composition. Although some of these statistically significant differences could be rare adventitious statistical associations resulting from the large number of comparisons being made,<sup>21</sup> the finding that these differences cluster in the domains of fat metabolism and blood composition argue that they are valid. Furthermore, sex-specific, genotype-related differences were discovered in body composition, indirect calorimetry, and macroscopic analyses of the heart and liver.

We found reduced lactate levels in Abcb5-deficient mice. Although this decrease is moderate, 1 mmol/L difference, and far from pathological, it could indicate a shift in cellular energy metabolism. For example, knockout of Mct4 or Mct1 lactate transporters results in a 6.7 mmol/L difference in plasma from pooled male and female mice or approximately 5 mmol/L differ-

ence in colon extracellular fluid from male mice. 22,23 It is important to note that mice and humans have different metabolisms represented by drastically different metabolic rates. Therefore, the magnitude of variation for several parameters observed in mice may be different in humans, as discussed by Sadaf Faroogi and colleagues regarding obesity in this model.<sup>24</sup> We did not observe any neurological alterations in the mice as a result of a putative cellular energy decline. Nonetheless, this could also be an effect of the age at the time of testing, and it might be different in older mice because a hypothesized energy deficit often progresses with aging. However, old Abcb5-deficient mice do not develop any visible signs of neurological disease over a two-year observation period. Increased anisocytosis was diagnosed in mutant mice, not accompanied by iron deficiency (Table \$15) but with decreased white blood cells (WBC) and platelet counts. These changes could account for the reduced lactate levels in the mutant mice. On the other hand, the Abcb5 transporter was found to be expressed in smooth muscles, though at a low level (CT values: 37.80; ΔCt: 30.62), and could also contribute to the reduced lactate level observed in Abcb5-deficient mice.

The clinical chemistry screen revealed lower triglycerides in ad libitum-fed mutant mice, as well as higher fasting total cholesterol and HDL cholesterol. No significant changes in non-HDL cholesterol were observed. Abcb5-deficient mice showed a reduced number of lipid droplets in the heart and a female specific decrease in lipid droplet number and size in the liver. Furthermore, we also found that female Abcb5-deficient mice had decreased fat content and increased lean mass, along with a trend toward an increase in maximum oxygen consumption, while in males, no difference between genotypes was observed. Interestingly, ABCB5 was found to be highly expressed in atherosclerotic plaques.<sup>25</sup> Furthermore, ABCB5 expression has been shown to be increased in atherosclerotic plaques of high-risk patients compared to low-risk patients when divided into two groups using ABCD2 and CAR scores.<sup>26</sup> Higher HDL levels, as observed in Abcb5-deficient mice, are



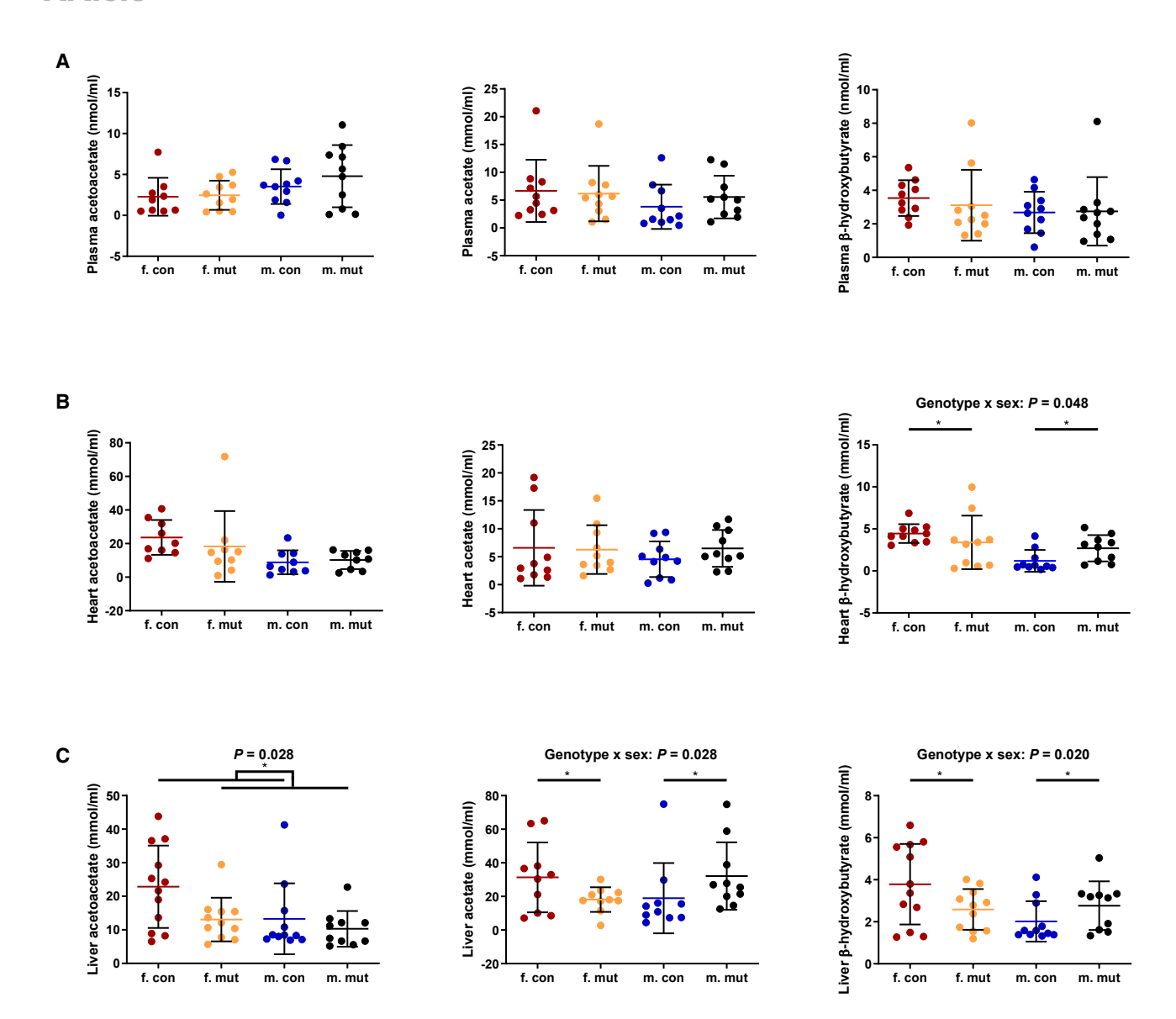


Figure 5. Variation of ketone bodies levels in Abcb5-mutant mice

Quantification of ketone bodies (acetoacetate, acetate,  $\beta$ -hydroxybutyrate) in the plasma (A), heart (B), and liver (C). Variations in acetoacetate levels were observed in the liver (p = 0.028) of Abcb5-knockout mice. A female-specific decrease and a male-specific increase in  $\beta$ -hydroxybutyrate levels was observed in heart (p = 0.048) and liver (p = 0.020). A similar observation was made for acetate levels in the liver (p = 0.028). Two cohorts, each consisting of 10 male and 10 female WT and homozygous mutant adult mice, all born within one week, were analyzed for ketone body levels at 8 weeks of age. Means, standard deviations, and p-values for genotype, sex, and genotype–sex interaction effects were calculated using a two-way ANOVA. \*p < 0.05, \*\*p < 0.01, \*\*\*p < 0.001. See Table 5.

known to be atheroprotective. <sup>27</sup> This suggests that Abcb5 does not play an atheroprotective role, unlike Abca1, which is involved in the export of cholesterol and phospholipids to HDL, which removes cholesterol from the bloodstream to prevent its accumulation in blood vessels. <sup>28</sup> Therefore, it can be hypothesized that Abcb5 transports cholesterol and contributes to atherogenesis, in contrast to Abca1. In our hands, ABCB5 ATPase activity in High-Five insect cell membrane vesicles was stimulated by cholesterol, but we were not able to demonstrate that this was mediated by cholesterol transport and not an indirect stimulation of ABCB5 ATPase activity (data not shown). For instance,

ABCB1 ATPase activity is stimulated by cholesterol through the modification of its lipid environment.<sup>29</sup> To further highlight the implication of Abcb5 in lipid homeostasis, ketone bodies were quantified in plasma, liver, and heart of Abcb5-deficient mice. Ketone bodies were decreased in the liver and heart of Abcb5-deficient females, whereas they were increased in the liver and heart of Abcb5-deficient males. Since ketone bodies are produced in the liver to supply energy to the heart, this explains the similar variation in both organs. Decreased ketone bodies can be explained by a decrease in fatty acid liver, the source of ketone production, as indicated by decreased



Estrogen	No	No	Yes	Yes
pSG5-ERα	No	Yes	Yes	Yes

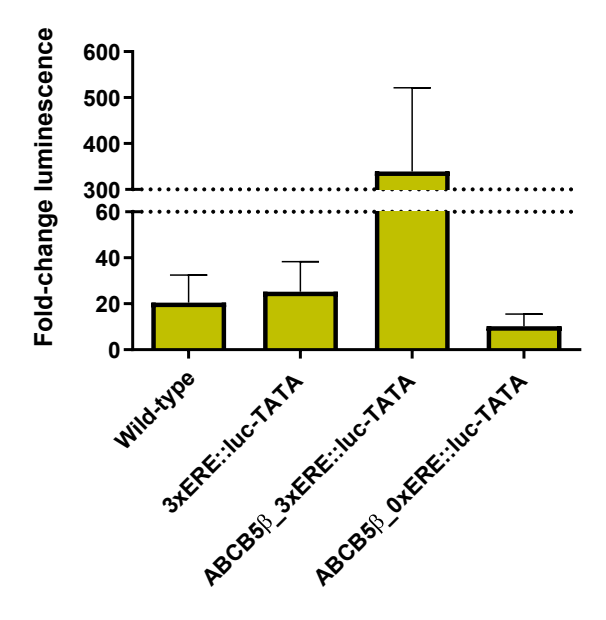


Figure 6. ER $\alpha$  activates ABCB5 $\beta$  transcription

MelJuSo were transfected with pSG5-hER $\alpha$  and either 3xERE::luc-TATA, ABCB5 $\beta$ \_3xERE::luc-TATA or ABCB5 $\beta$ \_0xERE::luc-TATA (n=6). 24 h post-transfection, cells were incubated with 5 mM estrogen. Then, luminescence was analyzed using the Dual-Luciferase Reporter Assay System (Promega). The y axis represents the luminescence fold change compared to MelJuSo transfected with pSG5 empty plasmid and 3xERE::luc-TATA in the absence of estrogen.

triglyceride levels and the number of lipid droplets in the liver. However, the opposite variation in both genders raises questions about the reason for such a pronounced sex difference in body composition. Estrogen-response elements (ERE) are found in the promoter region of Abcb5. Using a luciferase reporter assay, we have shown that ABCB5 $\beta$  expression is induced by human estrogen receptor  $\alpha$  in the presence of estrogen. This suggests that ABCB5 $\beta$  expression is regulated by hormones, explaining the important sex difference observed. In mice, Abcb1 expression has also been shown to be regulated by estrogen.<sup>30</sup>

The liver and heart were subjected to mRNA expression profiling because of phenotypic alterations identified in the metabolism, cardiovascular, and pathology screens. Among the differentially expressed genes in the liver, GO annotations have revealed those genes involved in the circadian clock<sup>31</sup> and lipid metabolism, which may link changes at the molecular level with the observed metabolic alterations and changes in body composition. In the heart, our analysis revealed genes involved with inflammation, atherosclerosis, blood pressure, cardiomyopathy, and other heart diseases, indicating clear alterations of cardiac functions at the molecular level. However, Abcb5 was not found to be expressed in WT liver and heart. Nevertheless, melanocyte-like cells have been identified in the heart. 32,33 Because ABCB5 is known to be predominantly expressed in pigmented cells, we hypothesize that the knockout of Abcb5 has an impact on the function of the heart by the disruption of the some unknown function of these melanocytic cells. Seven ABC transporters were found to be differentially expressed in the heart. Among those, six were upregulated in Abcb5-deficient mice, including Abca9 (2-fold), Abcb1a/b1b (4-fold), Abcg2 (2-fold), and Abcg4 (3-fold). Intriguingly, Abca8 was not found to be expressed in the hearts of Abcb5-mutant mice, yet it was in WT mice. ABCA8 has been shown to transport cholesterol and taurocholic acid.<sup>34</sup> The liver showed the greatest alterations in the Abc gene expression profile. Thirty-two transporters were overexpressed with a fold change greater than five. Among these transporters, several have been implicated in lipid homeostasis, particularly the Abca and Abcg transporters. For example, Abca1<sup>-/-</sup> and Abcg1<sup>-/-</sup> mice show increased lipid deposition in various tissues. 35,36 Their upregulation in Abcb5-deficient mice suggests that they compensate for the absence of Abcb5 to restore normal lipid metabolism. Furthermore, Abcb5 knockout is accompanied by the overexpression of a wide range of Abc transporters in five out of the seven tissues examined. It is important to note that, with a few exceptions, Abca and Abcg transporters are not differentially expressed in tissues other than the liver, suggesting a lesser impact of Abcb5 knockout on lipid metabolism in these organs.

Different methods were employed to analyze the eyes of Abcb5-deficient mice compared with their control littermates. The mice were examined for anterior segment abnormalities

Table 6. Concentration of steroid hormones in plasma of female and male Abcb5 WT and Abcb5 KO mice Female Male WT WT KO KO N = 5N = 9N = 7N = 10Female Male Overall Median [25%, 75%] p-value Corticosterone 663.86 [580.15, 707.15] 666.74 [502.22, 750.45] 83.7 [55.71, 103.33] 108.96 [80.24, 0.823 0.161 0.441 [mmol/L] 129.6] Androstenedione 0.4 [0.4, 0.4] 0.4 [0.4, 0.4] 0.4 [0.4, 0.51] 0.4 [0.4, 0.4] NA 0.434 0.451 [mmol/L] Testosterone 0.4 [0.4, 0.4] 0.4 [0.4, 0.4] 2.39 [0.94, 13.94] 5.37 [2.99, 8.45] 0.357 0.315 [mmol/L]

Medians, first and third quartiles and p-values calculated by a Wilcoxon rank-sum test.





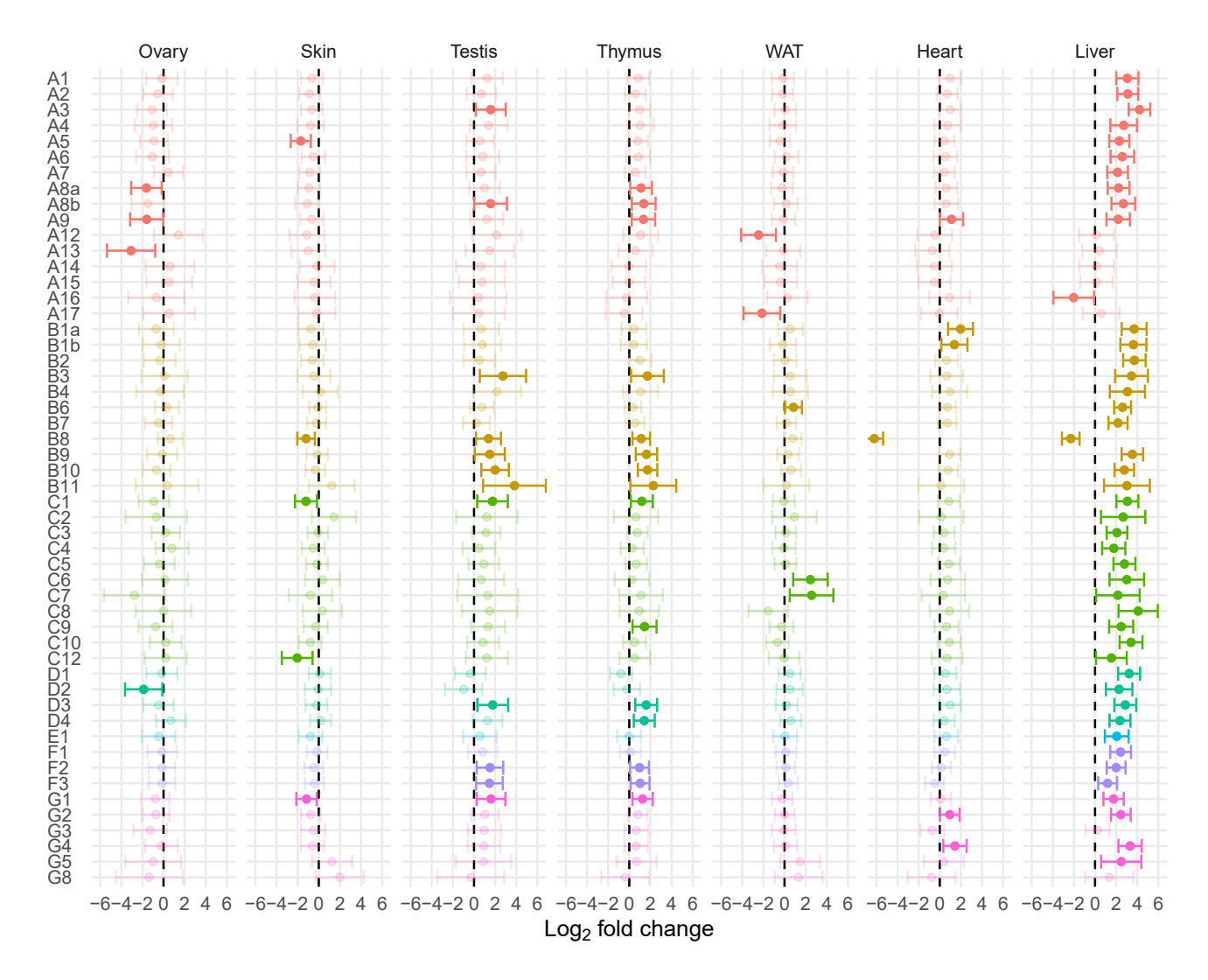


Figure 7. Differential Abc gene expression profile in Abcb5-knockout mice

Representation of the impact of Abcb5 KO on the expression of other Abc genes in seven different organs. Points and error bars represent geometric means and 95% confidence intervals on the mean, respectively. Statistical significance is represented using darker dots. The mRNA expression profile of 52 murine Abc transporters was measured in seven tissues collected from 5 male and 5 female WT and homozygous mutant adult mice, all born within one week, and analyzed at 12 weeks of age.

by slit lamp biomicroscopy, as well as for posterior segment abnormalities by fundoscopy. These examinations revealed transparent corneas and lenses and a regularly developed fundus in Abcb5-mutant mice. When the mice were sacrificed for pathological examinations, the eyes were fixed for histological analysis, which did not reveal any alteration in retinal lamination or the morphology of cell layers and lens. Ksander et al. reported an Abcb5 knockout mouse generated by the deletion of exon 10 of the gene in the C57BL/6J mouse strain. This knockout of the putative isoform B5X0E4-2 corresponds to the human ABCB5β. In this previous study, Abcb5-deficient mice were indistinguishable by physical examination from their WT littermates through adulthood, and their eyes contained all anterior and posterior segment components. However, histological analysis of their corneas demonstrated developmental

abnormalities characterized by decreased cellularity of the apical epithelial layer and disorganized basal and wing cell layers, which we did not observe in the Abcb5 knockout mice generated in our work. The Abcb5-deficient mouse model described in our work was generated by the deletion of exon 2 of the gene, which led to the knockout of both isoforms currently reported in databases. The RT-qPCR that we performed used a TaqMan probe that could recognize both isoforms. It is possible that the Abcb5 knockout reported by Ksander et al. does not completely the abrogate expression of both isoforms of Abcb5, accounting for this phenotypic difference. Exon 10 encodes protein sequence 357 to 394, which is found in the helix 6 region going into NBD1 (see Figure S1).

In a collaborative study, we have previously reported that the Abcb5 knockout mice studied here show evidence of



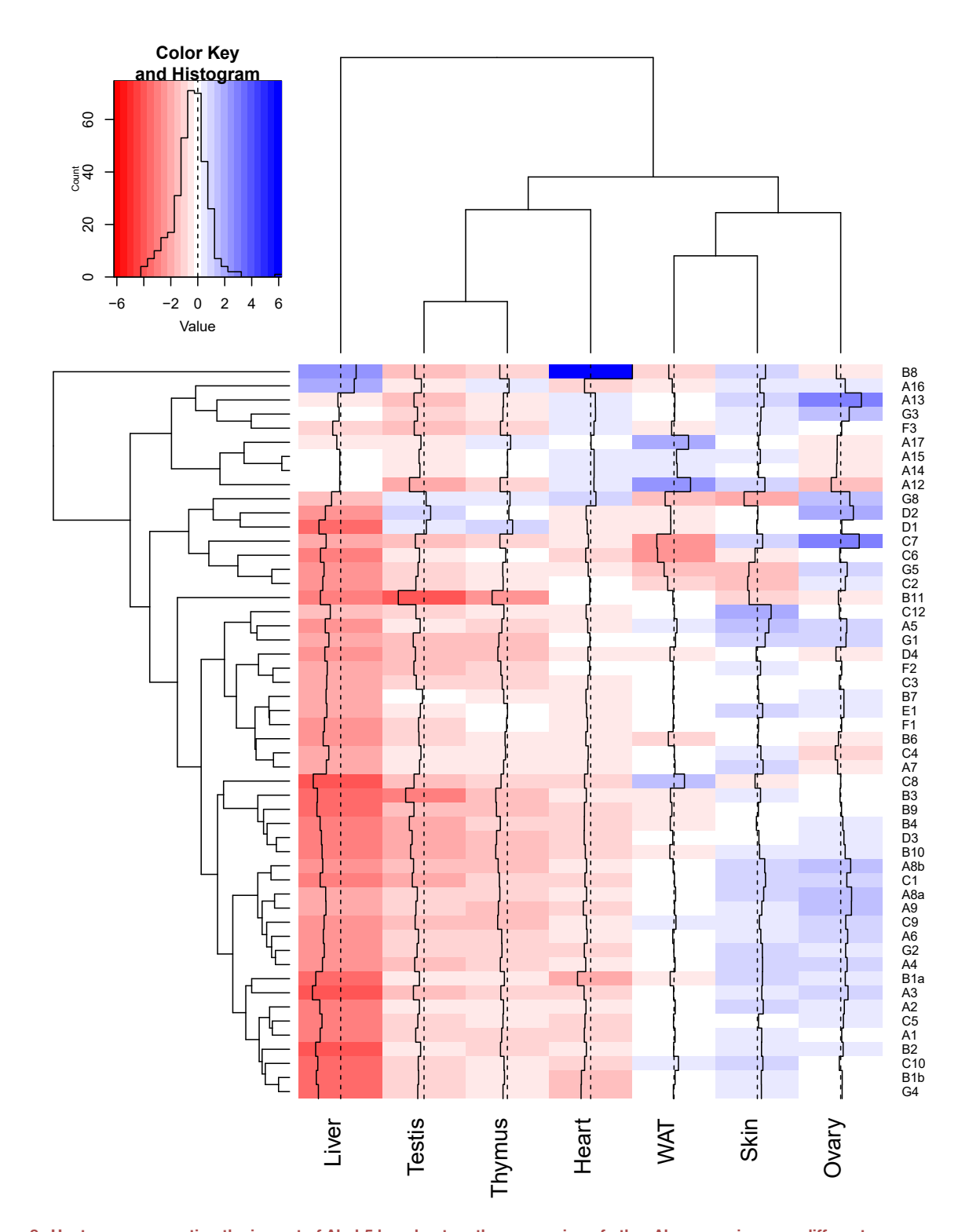


Figure 8. Heatmap representing the impact of Abcb5 knockout on the expression of other Abc genes in seven different organs

Tile colors represent the  $\Delta\Delta$ Ct values. Low  $\Delta\Delta$ Ct corresponds to overexpression and is red colored. Genes and organs are clustered following the Euclidean distance; data are not scaled. The mRNA expression profile of 52 murine ABC transporters was measured in seven tissues collected from 5 male and 5 female WT and homozygous mutant adult mice, all born within one week, and analyzed at 12 weeks of age.



decreased haloperidol effects in their brains.<sup>37</sup> This previous study suggests that the knockout mice may show altered susceptibility to other pharmacologic agents that are transported by the ABCB5 transporter, but this possibility has not yet been explored in detail.

Here, we report the complete pathological, behavioral, and metabolic phenotyping of Abcb5-deficient mice in collaboration with the GMC. The mice were fertile and demonstrated altered bioenergetics and fat metabolism, along with alterations in the blood composition. This study points to previously unrecognized avenues of investigation into the role of Abcb5 in intermediary metabolism, especially in the context of atherogenesis.

#### **Limitations of the study**

Although knockout mice represent powerful models to study the function of a gene in a living animal, the knocking out of a gene in mice may produce different changes than those that would be observed in humans in which the same gene was inactivated. We believe that the current study provides several new pieces of the jigsaw puzzle that hint toward a global role of ABCB5 in intermediary metabolism. However, further studies are required to fully understand the exact role of this ABC transporter in this very complex metabolic pathway.

#### **RESOURCE AVAILABILITY**

#### **Lead contact**

Requests for further information and resources should be directed to and will be fulfilled by the lead contact, Jean-Pierre Gillet (jean-pierre.gillet@unamur.be).

#### **Materials availability**

All unique/stable reagents generated in this study are available from the lead contact with a completed materials transfer agreement. Abcb5-knockout mice generated in this study were preserved through sperm cryopreservation and can be requested from the Laboratory of Molecular Cancer Biology, URPhyM, NARILIS, Faculty of Medicine, University of Namur, 5000 Namur, Belgium, or the Laboratory of Cell Biology, Center for Cancer Research, National Cancer Institute, NIH, 20892-4256 Bethesda, MD, USA. We are happy to share sperm straws upon request, provided that the requester covers the costs of processing and shipping.

#### Data and code availability

- The data reported in this article will be shared by the lead contact upon request. Expression data are available in the public repository GEO, and the accession number is provided in the key resources table.
- This article does not report original code.
- Any additional information required to reanalyze the data reported in this
  article is available from the lead contact upon request.

#### **ACKNOWLEDGMENTS**

This study was supported by the German Federal Ministry of Education and Research (Infrafrontier grant 01KX1012 to MHA) and the German Center for Diabetes Research (DZD) (MHA). We thank Michel Savels (URPhyM, NARILIS) for his help with the artwork. We thank Prof. René Rezsohazy (LIBST, UCLouvain) for sharing the pSG5-hER $\alpha$  and 3xERE:luc-TATA plasmids. This research was supported [in part] by the Intramural Research Program of the NIH.

#### **AUTHOR CONTRIBUTIONS**

J.-P.G. and M.M.G. designed the experiments and supervised the study. E. S. and L.T. generated conditional Abcb5 knockout mice. J.-P.G., W.V., and M.F. backcrossed the mice and generated the cohorts for phenotyping. F.G. and M.F. carried out the experiments to assess the compensation mechanism through ABC transporter upregulation, and B.B. performed statistical analysis of the data. B.R., J.R., T.K.-R., L.B., A.A.-P., M.H., N.S., C.P., M. F., and L.G. performed the experiments investigating the phenotype of the mice. J.B., V.G.-D., H.F., and M.H.A. supervised the mouse study and conceived the phenotypic tests. J.-P.G., M.M.G., and L.G wrote the article.

#### **DECLARATION OF INTERESTS**

The authors declare no competing financial interests.

#### **STAR+METHODS**

Detailed methods are provided in the online version of this paper and include the following:

- KEY RESOURCES TABLE
- EXPERIMENTAL MODEL AND STUDY PARTICIPANT DETAILS
  - Animal studies
- METHOD DETAILS
  - o ABCB5 modeling
  - o Genomic DNA extraction
  - o Abcb5-knockout mice
  - O Abcb5-knockout mice phenotyping
  - Lipid droplets staining
  - o Ketone bodies levels quantification
  - Luciferase reporter assay
  - Abc transporter gene expression profiling using TaqMan-based RTqPCR
- QUANTIFICATION AND STATISTICAL ANALYSIS

#### SUPPLEMENTAL INFORMATION

Supplemental information can be found online at https://doi.org/10.1016/j.isci. 2025.113617.

Received: April 21, 2022 Revised: May 19, 2025 Accepted: September 18, 2025 Published: September 20, 2025

#### REFERENCES

- Thomas, C., and Tampé, R. (2020). Structural and Mechanistic Principles of ABC Transporters. Annu. Rev. Biochem. 89, 605–636. https://doi.org/ 10.1146/annurev-biochem-011520-105201.
- Frank, N.Y., Pendse, S.S., Lapchak, P.H., Margaryan, A., Shlain, D., Doeing, C., Sayegh, M.H., and Frank, M.H. (2003). Regulation of progenitor cell fusion by ABCB5 P-glycoprotein, a novel human ATP-binding cassette transporter. J. Biol. Chem. 278, 47156–47165. https://doi.org/10.1074/ibc.M308700200.
- Kawanobe, T., Kogure, S., Nakamura, S., Sato, M., Katayama, K., Mitsuhashi, J., Noguchi, K., and Sugimoto, Y. (2012). Expression of human ABCB5 confers resistance to taxanes and anthracyclines. Biochem. Biophys. Res. Commun. 418, 736–741. https://doi.org/10.1016/j.bbrc.2012.01.090.
- Chen, K.G., Szakács, G., Annereau, J.P., Rouzaud, F., Liang, X.J., Valencia, J.C., Nagineni, C.N., Hooks, J.J., Hearing, V.J., and Gottesman, M.M. (2005). Principal expression of two mRNA isoforms (ABCB 5alpha and ABCB 5beta) of the ATP-binding cassette transporter gene ABCB 5 in



- melanoma cells and melanocytes. Pigment Cell Res. 18, 102–112. https://doi.org/10.1111/j.1600-0749.2005.00214.x.
- Keniya, M.V., Holmes, A.R., Niimi, M., Lamping, E., Gillet, J.P., Gottesman, M.M., and Cannon, R.D. (2014). Drug resistance is conferred on the model yeast Saccharomyces cerevisiae by expression of full-length melanomaassociated human ATP-binding cassette transporter ABCB5. Mol. Pharm. 11, 3452–3462. https://doi.org/10.1021/mp500230b.
- Moitra, K., Im, K., Limpert, K., Borsa, A., Sawitzke, J., Robey, R., Yuhki, N., Savan, R., Huang, D.W., Lempicki, R.A., et al. (2012). Differential gene and microRNA expression between etoposide resistant and etoposide sensitive MCF7 breast cancer cell lines. PLoS One 7, e45268. https://doi.org/ 10.1371/journal.pone.0045268.
- Schatton, T., Murphy, G.F., Frank, N.Y., Yamaura, K., Waaga-Gasser, A. M., Gasser, M., Zhan, Q., Jordan, S., Duncan, L.M., Weishaupt, C., et al. (2008). Identification of cells initiating human melanomas. Nature 451, 345–349. https://doi.org/10.1038/nature06489.
- Luo, Y., Ellis, L.Z., Dallaglio, K., Takeda, M., Robinson, W.A., Robinson, S. E., Liu, W., Lewis, K.D., McCarter, M.D., Gonzalez, R., et al. (2012). Side population cells from human melanoma tumors reveal diverse mechanisms for chemoresistance. J. Invest. Dermatol. 132, 2440–2450. https://doi.org/10.1038/ijd.2012.161.
- Ksander, B.R., Kolovou, P.E., Wilson, B.J., Saab, K.R., Guo, Q., Ma, J., McGuire, S.P., Gregory, M.S., Vincent, W.J.B., Perez, V.L., et al. (2014). ABCB5 is a limbal stem cell gene required for corneal development and repair. Nature 511, 353–357. https://doi.org/10.1038/nature13426.
- Sana, G., Madigan, J.P., Gartner, J.J., Fourrez, M., Lin, J., Qutob, N., Narayan, J., Shukla, S., Ambudkar, S.V., Xia, D., et al. (2019). Exome sequencing of ABCB5 identifies recurrent melanoma mutations that result in increased proliferative and invasive capacities. J. Invest. Dermatol. 139, 1985–1992.e10. https://doi.org/10.1016/j.jid.2019.01.036.
- Kondo, S., Hongama, K., Hanaya, K., Yoshida, R., Kawanobe, T., Katayama, K., Noguchi, K., and Sugimoto, Y. (2015). Upregulation of cellular glutathione levels in human ABCB5- and murine Abcb5-transfected cells. BMC Pharmacol. Toxicol. 16, 37. https://doi.org/10.1186/s40360-015-0038-5.
- Liu, P., Jenkins, N.A., and Copeland, N.G. (2003). A highly efficient recombineering-based method for generating conditional knockout mutations. Genome Res. 13, 476–484. https://doi.org/10.1101/gr.749203.
- Tessarollo, L., Palko, M.E., Akagi, K., and Coppola, V. (2009). Gene targeting in mouse embryonic stem cells. Methods Mol. Biol. 530, 141–164. https://doi.org/10.1007/978-1-59745-471-1\_8.
- Southon, E., and Tessarollo, L. (2009). Manipulating mouse embryonic stem cells. Methods Mol. Biol. 530, 165–185. https://doi.org/10.1007/ 978-1-59745-471-1\_9.
- Reid, S.W., and Tessarollo, L. (2009). Isolation, microinjection and transfer of mouse blastocysts. Methods Mol. Biol. 530, 269–285. https://doi.org/ 10.1007/978-1-59745-471-1\_14.
- Fuchs, H., Gailus-Durner, V., Adler, T., Aguilar-Pimentel, J.A., Becker, L., Calzada-Wack, J., Da Silva-Buttkus, P., Neff, F., Götz, A., Hans, W., et al. (2011). Mouse phenotyping. Methods 53, 120–135. https://doi.org/ 10.1016/j.ymeth.2010.08.006.
- Gailus-Durner, V., Fuchs, H., Adler, T., Aguilar Pimentel, A., Becker, L., Bolle, I., Calzada-Wack, J., Dalke, C., Ehrhardt, N., Ferwagner, B., et al. (2009). Systemic first-line phenotyping. Methods Mol. Biol. 530, 463–509. https://doi.org/10.1007/978-1-59745-471-1\_25.
- Gailus-Durner, V., Fuchs, H., Becker, L., Bolle, I., Brielmeier, M., Calzada-Wack, J., Elvert, R., Ehrhardt, N., Dalke, C., Franz, T.J., et al. (2005). Introducing the German Mouse Clinic: open access platform for standardized phenotyping. Nat. Methods 2, 403–404. https://doi.org/10.1038/nmeth0605-403.
- Papazafiropoulou, A.K., Georgopoulos, M.M., and Katsilambros, N.L. (2021). Ketone bodies and the heart. Arch. Med. Sci. Atheroscler. Dis. 6, e209–e214. https://doi.org/10.5114/amsad.2021.112475.

- Gerard, L., Duvivier, L., Fourrez, M., Salazar, P., Sprimont, L., Xia, D., Ambudkar, S.V., Gottesman, M.M., and Gillet, J.P. (2024). Identification of two novel heterodimeric ABC transporters in melanoma: ABCB5β/B6 and ABCB5β/B9. J. Biol. Chem. 300, 105594. https://doi.org/10.1016/j.jbc. 2023.105594.
- Armstrong, R.A. (2014). When to use the Bonferroni correction.
   Ophthalmic Physiol. Opt. 34, 502–508. https://doi.org/10.1111/opo. 12131.
- Smith, S., Witkowski, A., Moghul, A., Yoshinaga, Y., Nefedov, M., de Jong, P., Feng, D., Fong, L., Tu, Y., Hu, Y., et al. (2012). Compromised mitochondrial fatty acid synthesis in transgenic mice results in defective protein lipoylation and energy disequilibrium. PLoS One 7, e47196. https://doi.org/10.1371/journal.pone.0047196.
- Wang, S., Zhang, L., Zhao, J., Bai, M., Lin, Y., Chu, Q., Gong, J., Qiu, J., and Chen, Y. (2024). Intestinal monocarboxylate transporter 1 mediates lactate transport in the gut and regulates metabolic homeostasis of mouse in a sex-dimorphic pattern. Life Metab. 3, load041. https://doi.org/10. 1093/lifemeta/load041.
- Farooqi, I.S., and Xu, Y. (2024). Translational potential of mouse models of human metabolic disease. Cell 187, 4129–4143. https://doi.org/10.1016/j. cell.2024.07.011.
- Kotlyarov, S., and Kotlyarova, A. (2021). Analysis of ABC Transporter Gene Expression in Atherosclerosis. Cardiogenetics 11, 204–218. https://doi. org/10.3390/cardiogenetics11040021.
- Waden, K., Karlof, E., Narayanan, S., Lengquist, M., Hansson, G.K., Hedin, U., Roy, J., and Matic, L. (2022). Clinical risk scores for stroke correlate with molecular signatures of vulnerability in symptomatic carotid patients. iScience 25, 104219. https://doi.org/10.1016/j.isci.2022.104219.
- Hoekstra, M., and Van Eck, M. (2015). Mouse models of disturbed HDL metabolism. Handb. Exp. Pharmacol. 224, 301–336. https://doi.org/10. 1007/978-3-319-09665-0\_9.
- Ogura, M. (2022). HDL, cholesterol efflux, and ABCA1: Free from good and evil dualism. J. Pharmacol. Sci. 150, 81–89. https://doi.org/10.1016/j.jphs. 2022.07.004.
- Fenyvesi, F., Fenyvesi, E., Szente, L., Goda, K., Bacsó, Z., Bácskay, I., Váradi, J., Kiss, T., Molnár, E., Janáky, T., et al. (2008). P-glycoprotein inhibition by membrane cholesterol modulation. Eur. J. Pharm. Sci. 34, 236–242. https://doi.org/10.1016/j.ejps.2008.04.005.
- Kanado, Y., Tsurudome, Y., Omata, Y., Yasukochi, S., Kusunose, N., Akamine, T., Matsunaga, N., Koyanagi, S., and Ohdo, S. (2019). Estradiol regulation of P-glycoprotein expression in mouse kidney and human tubular epithelial cells, implication for renal clearance of drugs. Biochem. Biophys. Res. Commun. 519, 613–619.
- Pacha, J., Balounova, K., and Sotak, M. (2021). Circadian regulation of transporter expression and implications for drug disposition. Expert Opin. Drug Metab. Toxicol. 17, 425–439. https://doi.org/10.1080/ 17425255.2021.1868438.
- Levin, M.D., Lu, M.M., Petrenko, N.B., Hawkins, B.J., Gupta, T.H., Lang, D., Buckley, P.T., Jochems, J., Liu, F., Spurney, C.F., et al. (2009). Melanocyte-like cells in the heart and pulmonary veins contribute to atrial arrhythmia triggers. J. Clin. Investig. 119, 3420–3436. https://doi.org/10.1172/JCl39109.
- Mjaatvedt, C.H., Kern, C.B., Norris, R.A., Fairey, S., and Cave, C.L. (2005).
   Normal distribution of melanocytes in the mouse heart. Anat. Rec. A Discov. Mol. Cell. Evol. Biol. 285, 748–757. https://doi.org/10.1002/ar.a.
- Sasaki, K., Tachikawa, M., Uchida, Y., Hirano, S., Kadowaki, F., Watanabe, M., Ohtsuki, S., and Terasaki, T. (2018). ATP-Binding Cassette Transporter A Subfamily 8 Is a Sinusoidal Efflux Transporter for Cholesterol and Taurocholate in Mouse and Human Liver. Mol. Pharm. 15, 343–355. https://doi.org/10.1021/acs.molpharmaceut.7b00679.
- Christiansen-Weber, T.A., Voland, J.R., Wu, Y., Ngo, K., Roland, B.L., Nguyen, S., Peterson, P.A., and Fung-Leung, W.P. (2000). Functional



- loss of ABCA1 in mice causes severe placental malformation, aberrant lipid distribution, and kidney glomerulonephritis as well as high-density lipoprotein cholesterol deficiency. Am. J. Pathol. *157*, 1017–1029. https://doi.org/10.1016/S0002-9440(10)64614-7.
- Kennedy, M.A., Barrera, G.C., Nakamura, K., Baldán, A., Tarr, P., Fishbein, M.C., Frank, J., Francone, O.L., and Edwards, P.A. (2005). ABCG1 has a critical role in mediating cholesterol efflux to HDL and preventing cellular lipid accumulation. Cell Metab. 1, 121–131. https://doi.org/10.1016/j. cmet.2005.01.002.
- Zheng, M., Zhang, H., Dill, D.L., Clark, J.D., Tu, S., Yablonovitch, A.L., Tan, M.H., Zhang, R., Rujescu, D., Wu, M., et al. (2015). The role of Abcb5 alleles in susceptibility to haloperidol-induced toxicity in mice and humans. PLoS Med. 12, e1001782. https://doi.org/10.1371/journal. pmed.1001782.
- Esser, L., Zhou, F., Pluchino, K.M., Shiloach, J., Ma, J., Tang, W.K., Gutierrez, C., Zhang, A., Shukla, S., Madigan, J.P., et al. (2017). Structures of the Multidrug Transporter P-glycoprotein Reveal Asymmetric ATP Binding and the Mechanism of Polyspecificity. J. Biol. Chem. 292, 446–461. https://doi.org/10.1074/jbc.M116.755884.
- Emsley, P., and Cowtan, K. (2004). Coot: model-building tools for molecular graphics. Acta Crystallogr. D Biol. Crystallogr. 60, 2126–2132. https://doi.org/10.1107/S0907444904019158.
- Murshudov, G.N., Vagin, A.A., and Dodson, E.J. (1997). Refinement of macromolecular structures by the maximum-likelihood method. Acta Crystallogr. D Biol. Crystallogr. 53, 240–255. https://doi.org/10.1107/ S0907444996012255.
- DeLano, W.L. (2002). Pymol: An Open-Source Molecular Graphics Tool. CCP4 Newsl. Protein Crystallogr. 40, 82–92.
- Moreth, K., Fischer, R., Fuchs, H., Gailus-Durner, V., Wurst, W., Katus, H. A., Bekeredjian, R., and Hrabě de Angelis, M. (2014). High-throughput phenotypic assessment of cardiac physiology in four commonly used inbred mouse strains. J. Comp. Physiol. B 184, 763–775. https://doi.org/10.1007/s00360-014-0830-3.

- Roth, D.M., Swaney, J.S., Dalton, N.D., Gilpin, E.A., and Ross, J., Jr. (2002). Impact of anesthesia on cardiac function during echocardiography in mice. Am. J. Physiol. Heart Circ. Physiol. 282, H2134–H2140. https://doi.org/10.1152/ajpheart.00845.2001.
- Sahn, D.J., DeMaria, A., Kisslo, J., and Weyman, A. (1978). Recommendations regarding quantitation in M-mode echocardiography: results of a survey of echocardiographic measurements. Circulation 58, 1072–1083.
- Horsch, M., Schädler, S., Gailus-Durner, V., Fuchs, H., Meyer, H., de Angelis, M.H., and Beckers, J. (2008). Systematic gene expression profiling of mouse model series reveals coexpressed genes. Proteomics 8, 1248–1256. https://doi.org/10.1002/pmic.200700725.
- Kugler, J.E., Horsch, M., Huang, D., Furusawa, T., Rochman, M., Garrett, L., Becker, L., Bohla, A., Hölter, S.M., Prehn, C., et al. (2013). High mobility group N proteins modulate the fidelity of the cellular transcriptional profile in a tissue- and variant-specific manner. J. Biol. Chem. 288, 16690–16703. https://doi.org/10.1074/jbc.M113.463315.
- Saeed, A.I., Sharov, V., White, J., Li, J., Liang, W., Bhagabati, N., Braisted, J., Klapa, M., Currier, T., Thiagarajan, M., et al. (2003). TM4: a free, opensource system for microarray data management and analysis. Biotechniques 34, 374–378.
- Tusher, V.G., Tibshirani, R., and Chu, G. (2001). Significance analysis of microarrays applied to the ionizing radiation response. Proc. Natl. Acad. Sci. USA 98, 5116–5121. https://doi.org/10.1073/pnas.091062498.
- Edgar, R., Domrachev, M., and Lash, A.E. (2002). Gene Expression Omnibus: NCBI gene expression and hybridization array data repository. Nucleic Acids Res. 30, 207–210.
- Rathkolb, B., Hans, W., Prehn, C., Fuchs, H., Gailus-Durner, V., Aigner, B., Adamski, J., Wolf, E., and Hrabë de Angelis, M. (2013). Clinical Chemistry and Other Laboratory Tests on Mouse Plasma or Serum. Curr. Protoc. Mouse Biol. 3, 69–100. https://doi.org/10.1002/978047 0942390.mo130043.





### **STAR**\*METHODS

#### **KEY RESOURCES TABLE**

REAGENT or RESOURCE	SOURCE	IDENTIFIER
Critical commercial assays		
Acetate assay kit	Abcam	ab204719
Acetoacetate assay kit	Abcam	ab180875
β-hydroxybutyrate assay kit	Abcam	ab83390
Dual-Luciferase Reporter Assay kit	Promega	E1910
Mouse Ref8 v2.0 Expression BeadChip	Illumina	BD-202-0202
Deposited data		
Gene expression analysis of liver and heart from wildtype and ABCB5 mutant mice	This paper	GSE57699
Experimental models: Cell lines		
MelJuSo melanoma cell line	LBMC-JPGillet	N/A
Experimental models: Organisms/strains		
Abcb5-deficient C57BL/6J mice (Abcb5 <sup>ΔE2/ΔE2</sup> )	LBMC-UNamur-JPGillet NCI Frederick-LTessarollo	N/A
Oligonucleotides		
Forward primer Pf 5'-CATACATTATCCCTTTCACAGG-3'	This paper	N/A
Reverse primer Pr 5'-CATTGAGCAATCTTCCCTTTAC-3'	This paper	N/A
Forward primer Pf <sub>KO</sub> : 5'-GTTAACTCCAACTCTCAGCTAAG-3'	This paper	N/A
Reverse primer Pr <sub>KO</sub> : 5'-CTCAACAATTTCTATAGCAATTACC-3'.	This paper	N/A
Abca1	ThermoFisher Scientific	Mm00442646_m1
Abca2	ThermoFisher Scientific	Mm00431553_m1
Abca3	ThermoFisher Scientific	Mm00550501_m1
Abca4	ThermoFisher Scientific	Mm00492004_m1
Abca5	ThermoFisher Scientific	Mm00461656_m1
Abca6	ThermoFisher Scientific	Mm00461636_m1
Abca7	ThermoFisher Scientific	Mm00497010_m1
Abca8a	ThermoFisher Scientific	Mm00462440_m1
Abca8b	ThermoFisher Scientific	Mm00457361_m1
Abca9	ThermoFisher Scientific	Mm00461704_m1
Abca12	ThermoFisher Scientific	Mm00613683_m1
Abca13	ThermoFisher Scientific	Mm00624342_m1
Abca14	ThermoFisher Scientific	Mm00509570_m1
Abca15	ThermoFisher Scientific	Mm00623451_m1
Abca16	ThermoFisher Scientific	Mm01163245_m1
Abca17	ThermoFisher Scientific	Mm01299670_m1
Abcb1a	ThermoFisher Scientific	Mm00440761_m1
Abcb1b	ThermoFisher Scientific	Mm00440736_m1
Abcb2	ThermoFisher Scientific	Mm00443188_m1
Abcb3	ThermoFisher Scientific	Mm00441668_m1
Abcb4	ThermoFisher Scientific	Mm00435630_m1
Abcb5	ThermoFisher Scientific	Mm01225815_m1
Abcb6	ThermoFisher Scientific	Mm00470049_m1
Abcb7	ThermoFisher Scientific	Mm01235258_m1
Abcb8	ThermoFisher Scientific	Mm00472410_m1
		(Continued on payt page)

(Continued on next page)



Continued		
REAGENT or RESOURCE	SOURCE	IDENTIFIER
Abcb9	ThermoFisher Scientific	Mm00498197_m1
Abcb10	ThermoFisher Scientific	Mm00497927_m1
Abcb11	ThermoFisher Scientific	Mm00445168_m1
Abcc1	ThermoFisher Scientific	Mm00456156_m1
Abcc2	ThermoFisher Scientific	Mm00496899_m1
Abcc3	ThermoFisher Scientific	Mm00551550_m1
Abcc4	ThermoFisher Scientific	Mm01226380_m1
Abcc5	ThermoFisher Scientific	Mm00443360_m1
Abcc6	ThermoFisher Scientific	Mm00497685_m1
Abcc7	ThermoFisher Scientific	Mm00445197_m1
Abcc8	ThermoFisher Scientific	Mm00803450_m1
Abcc9	ThermoFisher Scientific	Mm00441638_m1
Abcc10	ThermoFisher Scientific	Mm00467403_m1
Abcc12	ThermoFisher Scientific	Mm00556685_m1
Abcd1	ThermoFisher Scientific	Mm00431749_m1
Abcd2	ThermoFisher Scientific	Mm00496455_m1
Abcd3	ThermoFisher Scientific	Mm00436150_m1
Abcd4	ThermoFisher Scientific	Mm00436180_m1
Abce1	ThermoFisher Scientific	Mm00649858_m1
Abcf1	ThermoFisher Scientific	Mm01275245_m1
Abcf2	ThermoFisher Scientific	Mm00457400_g1
Abcf3	ThermoFisher Scientific	Mm00658695_m1
Abcg1	ThermoFisher Scientific	Mm00437390_m1
Abcg2	ThermoFisher Scientific	Mm00496364_m1
Abcg3	ThermoFisher Scientific	Mm00446072_m1
Abcg4	ThermoFisher Scientific	Mm00507250_m1
Abcg5	ThermoFisher Scientific	Mm00446249_m1
Abcg8	ThermoFisher Scientific	Mm00445970_m1
18S	ThermoFisher Scientific	Hs99999901_s1
Recombinant DNA		
Mus musculus BAC clone RP23-161L22 from 12	Genbank AC126277.3	chori.org
pSG5-hERα	LIBST, UCLouvain RRezsohazy	N/A
3xERE::luc-TATA	LIBST, UCLouvain RRezsohazy	N/A
ABCB5β_3xERE::luc-TATA	LBMC-UNamur JPGillet	N/A
ABCB5β_0xERE::luc-TATA	LBMC-UNamur JPGillet	N/A
Software and algorithms		
mageJ	https://imagej.net/ij/	https://imagej.net/ij/
R 3.3.3 and the <i>nlme</i> , <i>ggplot2</i> , and <i>gplots</i> packages for linear mixed models, graphical representation, and heatmap, respectively	This paper	The R Foundation for Statistical Computing, 2017

#### **EXPERIMENTAL MODEL AND STUDY PARTICIPANT DETAILS**

#### **Animal studies**

Abcb5-knockout mice were bred in a specific, pathogen-free facility with food and water *ad libitum*. All experimental procedures followed the National Institutes of Health Guidelines for animal care and use and were approved by the NCI-Frederick and NCI-CCR ACUC committees. Mice were phenotyped at the German Mouse Clinic (GMC). They were maintained in individually ventilated cages (IVC) with water and standard mouse chow (Altromin no. 1324), per the GMC housing conditions and German laws. All tests performed at the GMC were approved by the responsible authority of the Regierung von Oberbayern. Lipid droplets staining, ketone bodies levels quantification and Abc transporter gene expression profiling using TaqMan-based RT-qPCR were carried out at the





University of Namur in Belgium. The experimental protocol was conducted in compliance with the European Communities Council Directives for Animal Experiments (2010/63/EU, 86/609/EEC and 87/848/EEC) and was approved by the Animal Ethics Committee of the University of Namur (ethic project UN 22-388). Sex-specific, genotype-related differences were discovered in body composition, indirect calorimetry, and macroscopic analyses of the heart and liver.

#### **METHOD DETAILS**

#### **ABCB5** modeling

The construction of the ABCB5 3-Dimensional model was approached using the method of homology modeling considering the availability of the structures mouse ABCB1 (P-glycoprotein or P-gp) and high sequence identity between human ABCB5 and mouse ABCB1 showing a greater than 60% sequence identity. An accurate alignment between the human ABCB5 and mouse ABCB1 sequences was generated based on a multi-sequence alignment that includes various members of the ABCB family transporters. Based on this alignment, the structural model of ABCB5 was constructed manually using the structural model of mouse P-gp (PDB:5KPI)<sup>38</sup> as template by replacing residues of mouse ABCB1 with corresponding residues of ABCB5 in the molecular graphics program Coot.<sup>39</sup> The model was subsequently subject to energy minimization using the crystallographic refinement program Refmac.<sup>40</sup> The model was rendered as ribbon diagram in the program Pymol.<sup>41</sup>

#### **Genomic DNA extraction**

The mice were identified using ear punch. Tissues were incubated 5 minutes at 95°C in 200 μl of lysis buffer (50 mM KCl, 50 mM Tris-HCI (pH 8.0), 2.5 mM EDTA, 0.45% NP-40, 0.45% Tween-20). Then, 5 µl of proteinase K were added to the samples, which were incubated at 55°C O/N. Samples were incubated 5 minutes at 95°C and then centrifuged 5 minutes at 15,000 x g. For DNA precipitation, supernatants were transferred to fresh tubes with 200 μl isopropanol. Tubes were inverted four to five times and centrifuged 1 minute at 15,000 x g. Supernatants were discarded, and the pellets were resuspended in 200 μl 70% ethanol. Tubes were centrifuged 1 minute at 15,000 x g, and supernatants were discarded. The pellets were allowed to dry for 15 minutes at RT and then resuspended in 102 μl ddH<sub>2</sub>O and incubated at 65°C for 1 hour. Genomic DNA was then quantified using SpectraMax i3 (Molecular Devices, San Jose, CA, USA).

#### **Abcb5-knockout mice**

The presence of a distal loxP site in the genome was tested by PCR using the following pair of primers: forward primer Pf 5'-CATA CATTATCCCTTTCACAGG-3' and reverse primer Pr 5'-CATTGAGCAATCTTCCCTTTAC-3'. Amplification of the WT or mutant Abcb5 alleles resulted in bands of either 239 bp (WT) or 330 bp (recombined allele). The mice were routinely genotyped by isolating genomic DNA from ear tissue following ear punch, as explained in the above section. Using 100 ng of genomic DNA as the template, PCR was performed using the forward primer Pf<sub>KO</sub>: 5'-GTTAACTCCAACTCTCAGCTAAG-3' and the reverse primer Pr<sub>KO</sub>: 5'-CTCAACAATTTC TATAGCAATTACC-3'. The PCR parameters were as follows: 3 min initial denaturation at 94°C; 30 cycles: 30 seconds denaturation at 94°C, 30 seconds annealing at 56°C, and 45 seconds extension at 72°C; and 3 minutes final elongation at 72°C. Amplification of the WT or mutant Abcb5 alleles resulted in bands of either 512 bp (Abcb5<sup>-/-</sup>), or 118 bp (Abcb5<sup>-/-</sup>).

# Abcb5-knockout mice phenotyping

#### **Echocardiography**

Cardiac function was evaluated with transthoracic echocardiography in 15-week-old mice using a Vevo2100 Imaging System (VisualSonics Inc., Toronto Canada) with a 30 MHz probe. Echocardiograms were recorded as reported before. 42 Briefly, the day before the first examination, mouse chests were depilated using a topical depilatory agent. Examinations were performed on conscious animals to prevent anesthesia-related impairment of cardiac function. 43 Left ventricular dimension in systole (LVIDs) and diastole (LVIDd), systolic and diastolic interventricular septum thickness (IVSs, IVSd), and systolic and diastolic posterior wall thickness (LVPWs, LVPWd) were monitored in parasternal short axes view in M-mode. Dimensions and wall widths were measured according to the American Society of Echocardiography leading edge method, here in three consecutive beats. 44 Heart rate was determined from the cardiac cycles recorded on the M-mode tracing by using at least three consecutive systolic intervals. In addition, the respiratory rate was calculated by measuring three consecutive respiratory intervals. Qualitative and quantitative measurements were made offline using analytical software (VisualSonics Inc.).

#### Molecular phenotyping

Total RNA was extracted from the liver and heart of four male wild type and three to four Abcb5 mutant mice with the RNeasy mini kit (Qiagen). For gene expression profiling, Illumina Mouse Ref8 v2.0 Expression BeadChips were applied, as previously described. 45,46 Data normalization (cubic spline) and background corrections were performed with Illumina Genomestudio 2011.1. Statistical analysis identified differentially regulated genes between the mutant and wild type tissue when comparing single mutant values with the mean of four wild types (FDR < 10%, fold change > 1.5). 47,48 Expression data are available at the public repository database GEO (GSE57699). 49 http://www.ncbi.nlm.nih.gov/geo/query/acc.cgi?token=czyfwasqzrshjyh&acc=GSE57699.



#### Heart weight determination

During necropsy the heart weight was determined together with body weight and tibia length. Briefly, the mice were euthanized by  $CO_2$  inhalation, weighed, and opened from the ventral midline. Exsanguination was achieved by cutting the dorsal aorta. Prior to dissection, the heart was inspected for abnormalities. For excision, the heart was removed from the pericardial membrane, and the major vessels were cut through at the point they enter or exit the atria. Heart weight was obtained wet after blotting the organ on paper towels. Tibia length was determined from the left tibia of the mouse using a digital caliper "MarCal" (Mahr GmbH; Göttingen, Germany).

#### **Blood withdrawal and storage**

Blood samples were taken from isoflurane-anesthetized mice by puncturing the retro-bulbar sinus with nonheparinized glass capillaries (1.0 mm in diameter; Neolab; Munich, Germany). The time of sample collection was recorded in a work list. Blood taken after overnight food withdrawal was collected in heparinized sample tubes (Li-heparin, KABE; Nümbrecht, Germany; Art.No. 078028), blood samples collected from ad libitum-fed mice were divided into two portions. The major portion was collected in a heparinized tube (Li-heparin, KABE; Nümbrecht, Germany; Art.No. 078028). The smaller portion was collected (using the same capillary) in an EDTA-coated tube (KABE, Art.No 078035). Each tube was immediately inverted five times to achieve a homogeneous distribution of the anticoagulant. The samples collected from unfed mice were stored in a rack on ice, separated by centrifugation (10 min, 5000 g; 8°C, Biofuge fresco, Heraeus; Hanau, Germany) as soon as possible, and plasma was used for clinical chemical analysis. Heparinized blood collected from ad libitum-fed mice was left in a rack at room temperature for 1 to 2 hours. Afterwards, cells and plasma were separated by a centrifugation step (10 min, 5000 g; 8°C, Biofuge fresco, Heraeus; Hanau, Germany). Plasma was distributed between the immunology screen (30 mL), the allergy screen (30 mL), the clinical chemical screen (110 mL) and the steroid screen (50 mL), while the cell pellet was given to the immunology screen for FACS analysis. The plasma samples for clinical chemical analyses were transferred into Eppendorf tubes and either used immediately (plasma of unfed mice) or diluted 1:2 with aqua dest (ad libitum-fed mice). The solution was mixed for 10 seconds (Vortex genie, Scientific Industries; New York, USA) to prevent clotting and then centrifuged again for 10 min at 5000 g at 8°C. In addition, the clinical chemical screen received the EDTA blood samples for hematological investigations, which were placed on a rotary agitator at room temperature until analysis.

#### Clinical chemistry

The screen was performed using an Olympus AU 400 auto-analyzer and adapted reagents from Olympus (Hamburg, Germany), save for free fatty acids (nonesterified fatty acid, NEFA) that were measured using a kit from Wako Chemicals GmbH (NEFA-HR2, Wako Chemicals, Neuss, Germany), and Glycerol, which was measured using a kit from Randox Laboratories GmbH (Krefeld, Germany). In the primary screen, 18 different parameters were measured, including various enzyme activities, as well as plasma concentrations of specific substrates and electrolytes for ad libitum-fed mice (Pipeline 2, Table S1), while six measured parameters and one calculated value (blood lipid and glucose levels) were determined in samples derived from mice after overnight food withdrawal (Pipeline 1, Table S1).

#### Hematology

A volume of 50 mL EDTA-blood was used to measure basic hematological parameters with a blood analyzer, which has been carefully validated for analysis of mouse blood (ABC-Blutbild-Analyzer, Scil Animal Care Company GmbH; Viernheim, Germany). The number and size of red blood cells, white blood cells, and platelets were measured by electrical impedance and hemoglobin by spectrophotometry. Mean corpuscular volume (MCV), mean platelet volume (MPV), and red blood cell distribution width (RDW) were calculated directly from the cell volume measurements. The hematocrit (HCT) was assessed by multiplying the MCV with the red blood cell count. Mean corpuscular hemoglobin (MCH) and mean corpuscular hemoglobin concentrations (MCHC) were calculated from hemoglobin/red blood cells count (MCH) and hemoglobin/hematocrit (MCHC), respectively.

#### Second sample analysis

A second sample was collected three weeks after the first bleeding from all animals investigated in pipeline 2 (Table S1) to retest a subset of parameters to check the reproducibility of the first results, if requested, and to provide the steroid screen with plasma samples for their analyses.

#### Statistical analysis

If not stated otherwise, data generated by the German Mouse Clinic was analyzed using R. Genotype effects were assessed using Wilcoxon rank sum test, linear models, ANOVA or post hoc test depending on the assumed distribution of the parameter studied and the question addressed. A p-value <0.05 has been used as level of significance; a correction for multiple testing has not been performed.

#### Lipid droplets staining

Liver and heart were incubated in formol for 48 to 72 hours. The organs were washed in tap water for 1 hour and then incubated in sucrose 30% for 48 hours. The organs were then placed in OCT (361603E, Avantor, Radnor Township, Pennsylvania, USA) and sectioned using a cryostat. Sections were stained with Oil Red O from Sigma-Aldrich (Saint-Louis, Missouri, USA) according to the manufacturer's instructions. Staining was visualized using Olympus BX63 (Olympus, Shinjuk City, Tokyo, Japan) in fluorescence. Lipid droplet size and number were analyzed using ImageJ (tool: analyze particles), and three images from six different mice per condition (female and male, WT and KO) were counted. Droplets were analyzed separately by two blinded observers.





#### Ketone bodies levels quantification

Acetoacetate, acetate and  $\beta$ -hydroxybutyrate were quantified using an acetoacetate assay kit (ab180875), an acetate assay kit (ab204719) and a  $\beta$ -hydroxybutyrate assay kit (ab83390), from Abcam (Cambridge, United Kingdom) according to the manufacturer's instructions. Plasma, heart, and liver from WT and KO mice were analyzed. Samples (n=10) were deproteinized and each organ was divided into three equal parts for separate analysis of acetoacetate, acetate, and  $\beta$ -hydroxybutyrate concentrations.

#### Luciferase reporter assay

100,000 MelJuSo cells per well were plated in a 6-well plate and transfected with the following plasmids: 250 ng of pSG5-hER $\alpha$  or pSG5 empty plasmid, 250 ng of 3xERE::luc-TATA, ABCB5 $\beta$ \_3xERE::luc-TATA or ABCB5 $\beta$ \_0xERE::luc-TATA and 25 ng of normalization plasmid using JetPrime (Polyplus, Illkirch, France) according to the manufacturer's instructions. 24 hours post-transfection, cells were incubated with 5 mM estrogen (E8875, Sigma-Aldrich, Saint-Louis, Missouri, USA). 72 hours post-transfection, proteins were harvested using the lysis buffer from the Dual-Luciferase Reporter Assay kit (Promega, Madison, Wisconsin, USA). The same kit was used for luminescence analysis.

#### Abc transporter gene expression profiling using TaqMan-based RT-qPCR

Total RNA was prepared using the Trizol method (Invitrogen, Carlsbad, CA) and was quantified using SpectraMax i3 (Molecular Devices, San Jose, CA). Synthesis of complementary DNA (cDNA) from 2  $\mu$ g total RNA in a 20  $\mu$ L reaction volume was carried out using the High Capacity cDNA Reverse Transcription kit with ribonuclease inhibitor (Applied Biosystems, Foster City, CA), per the manufacturer's instructions. Expression levels of the 53 mouse Abc transporters were measured using TaqMan-based RT-qPCR, per the manufacturer's instructions (Table S16). Plates were run on a CFX-96 Touch (BioRad, Hercules, CA), per the manufacturer's instructions. Data analysis was performed using the  $\Delta\Delta$ Ct method and the 18s as the housekeeping gene. The  $\Delta$ Ct was defined as  $Ct_{GO} - Ct_{18s}$  and  $\Delta\Delta$ Ct was defined as  $\Delta Ct_{KO} - \Delta Ct_{WT}$ . The  $\Delta\Delta$ Ct was adjusted for sex using a linear mixed model incorporating random intercept for each individual. The fold change was then defined as  $2^{-\Delta\Delta Ct}$ . We used R 3.3.3 (The R Foundation for Statistical Computing, 2017) and the *nlme*, *ggplot2*, and *gplots* packages for linear mixed models, graphical representation, and heatmap, respectively.

#### **QUANTIFICATION AND STATISTICAL ANALYSIS**

Quantification methods and statistical analysis are described above. The statistical test used and the definition of statistical significance in each case is included in the figure legends. Data are presented as the mean  $\pm$  the standard deviation (SD), unless otherwise noted.